




RESEARCH ARTICLE

Neuraminidase is a host-directed approach to regulate neutrophil responses in sepsis and COVID-19

Rodrigo de Oliveira Formiga^{1,2,3}  | Flávia C. Amaral^{1,3} | Camila F. Souza¹ | Daniel A. G. B. Mendes^{1,3} | Carlos W. S. Wanderley⁴ | Cristina B. Lorenzini^{1,3} | Adara A. Santos^{1,3} | Juliana Antônia¹ | Lucas F. Faria¹ | Caio C. Natale^{1,3} | Nicholas M. Paula^{1,3} | Priscila C. S. Silva¹ | Fernanda R. Fonseca⁵ | Luan Aires^{1,3} | Nicoli Heck^{1,3} | Márick R. Starick^{1,3} | Celso M. Queiroz-Junior⁶ | Felipe R. S. Santos⁷  | Filipe R. O. de Souza⁶ | Vivian V. Costa⁶ | Shana P. C. Barroso⁸ | Alexandre Morrot^{9,10} | Johan Van Weyenbergh¹¹ | Regina Sordi¹ | Frederico Alisson-Silva¹² | Fernando Q. Cunha⁴  | Edroaldo L. Rocha^{1,3} | Sylvie Chollet-Martin¹³ | Maria Margarita Hurtado-Nedelec¹⁴ | Clémence Martin^{2,15} | Pierre-Régis Burgel^{2,15} | Daniel S. Mansur³ | Rosemeri Maurici⁵ | Matthew S. Macauley¹⁶ | André Báfica³ | Véronique Witko-Sarsat² | Fernando Spiller^{1,3}

Correspondence

Fernando Spiller, Department of Pharmacology, Federal University of Santa Catarina, Av. Prof. Henrique da Silva Fontes, 321—Trindade, Florianópolis, SC 88040-900, Brazil.
Email: spiller.farmaco@gmail.com

Funding information

This work was funded by FAPESP-SCRIPPS (FS; 15/50387-4), Howard Hughes Medical Institute—Early Career Scientist (AB; 55007412), National Institutes of Health Global Research Initiative Program (AB; TW008276), Fonds Wetenschappelijk Onderzoek (FWO; Grant G0D6817N), CAPES Computational Biology (DSM; 23038.010048/2013-27), CNPq/COVID-19 (AB; 401209/2020-2), CNPq/PQ Scholars (AB and DSM), CAPES/PrInt, Le programme de bourses d'excellence Eiffel and FAPESC Scholarship (DAGBM).

Abstract

Background and Purpose: Neutrophil overstimulation plays a crucial role in tissue damage during severe infections. Because pathogen-derived neuraminidase (NEU) stimulates neutrophils, we investigated whether host NEU can be targeted to regulate the neutrophil dysregulation observed in severe infections.

Experimental Approach: The effects of NEU inhibitors on lipopolysaccharide (LPS)-stimulated neutrophils from healthy donors or COVID-19 patients were determined by evaluating the shedding of surface sialic acids, cell activation, and reactive oxygen species (ROS) production. Re-analysis of single-cell RNA sequencing of respiratory tract samples from COVID-19 patients also was carried out. The effects of oseltamivir on sepsis and betacoronavirus-induced acute lung injury were evaluated in murine models.

Key Results: Oseltamivir and zanamivir constrained host NEU activity, surface sialic acid release, cell activation, and ROS production by LPS-activated human neutrophils. Mechanistically, LPS increased the interaction of NEU1 with matrix metalloproteinase 9 (MMP-9). Inhibition of MMP-9 prevented LPS-induced NEU activity and neutrophil response. In vivo, treatment with oseltamivir fine-tuned neutrophil migration

Abbreviations: BAL, bronchoalveolar lavage; CpNEU, *Clostridium perfringens* neuraminidase; NETs, neutrophil extracellular traps; NEU, neuraminidase; OZ, opsonized zymosan; PL, peritoneal lavage; Sia, sialic acid.

For affiliations refer to page 18

and improved infection control as well as host survival in peritonitis and pneumonia sepsis. NEU1 also is highly expressed in neutrophils from COVID-19 patients, and treatment of whole-blood samples from these patients with either oseltamivir or zanamivir reduced neutrophil overactivation. Oseltamivir treatment of intranasally infected mice with the mouse hepatitis coronavirus 3 (MHV-3) decreased lung neutrophil infiltration, viral load, and tissue damage.

Conclusion and Implications: These findings suggest that interplay of NEU1–MMP-9 induces neutrophil overactivation. In vivo, NEU may serve as a host-directed target to dampen neutrophil dysfunction during severe infections.

KEYWORDS

COVID-19, metalloproteinase-9, neuraminidase, neutrophil, oseltamivir, SARS-CoV-2, sepsis, sialic acid, zanamivir

1 | INTRODUCTION

Neutrophils are key components of the immune response against pathogens (Mócsai, 2013). During severe acute infections, such as sepsis and COVID-19, overactivated neutrophils infiltrate vital organs and release cytotoxic molecules including proteases, reactive oxygen species (ROS), and neutrophil extracellular traps (NETs) (Alves-Filho et al., 2010; Veras et al., 2020). Although such inflammatory mediators are essential for infection control, they may damage healthy cells also (Segal, 2005). Therefore, the function of neutrophils must be regulated to efficiently clear microorganisms with minimal host detrimental effects.

Several mechanisms controlling neutrophil activation have been described (Steevels & Meyaard, 2011). For instance, the density of cell surface **sialic acid** (Sia) has been demonstrated to regulate leukocyte activation in response to microbial stimuli (Macauley et al., 2014). The dense array of Sia in the glycocalyx of all mammalian cells makes this monosaccharide a central molecule for many cellular processes including cell–cell interactions, signal transduction and transendothelial migration (Varki, 2008). Neuraminidases (NEUs) are enzymes found in pathogen and mammalian hosts, where they hydrolyse Sia residues linked to **galactose**, *N*-acetylgalactosamine or polySia residues on glycoconjugates, thereby regulating many physiological and pathological responses (Lipničanová et al., 2020). In human neutrophils, shedding of surface Sia by microbial-derived NEU leads to cellular activation, ROS production, and release of NETs (Arora & Henrichon, 1994; Chang et al., 2012; Henricks et al., 1982; Suzuki et al., 1982). Additionally, it has been demonstrated that **lipopolysaccharide (LPS)** induces host membrane-associated NEU activation in murine or human macrophages and dendritic cells (Amith et al., 2009). Upon LPS binding to **toll-like receptor 4 (TLR4)**, the **matrix metalloproteinase 9 (MMP-9)** triggers NEU activity and contributes to NFκB-induced responses in macrophages, suggesting a role for these enzymes during cell activation (Abdulkhalek et al., 2011; Amith et al., 2009). In Gram-negative experimental sepsis, leukocyte dysfunction also is mediated

What is already known

- Shedding of surface sialic acids by pathogen-derived neuraminidase leads to leukocyte activation.

What does this study add

- Interplay of host neuraminidases-matrix metalloproteinase (MMP)-9 trigger neutrophil activation.

What is the clinical significance

- Our findings highlight neuraminidases as host-directed targets to control neutrophil overactivation in sepsis and COVID-19.

by NEU activity and is associated with an exacerbated inflammatory response and high mortality rates (Chen et al., 2014; Yang et al., 2018). Because previous studies have demonstrated that pathogen-derived NEU stimulates neutrophils (Chang et al., 2012; Mills et al., 1981; Suzuki et al., 1982), we investigated whether endogenous NEU can be targeted to regulate neutrophil dysfunction observed in severe infections.

Here, we have identified host NEU as a positive regulator of microbial-induced human neutrophil overactivation, by a mechanism dependent on MMP-9 activity. Additionally, we have employed clinically available antiviral NEU inhibitors, **oseltamivir** and zanamivir, to explore this pathway and found that these drugs may represent valuable tools to fine-tune the neutrophil response in sepsis and COVID-19.

2 | METHODS

2.1 | Human blood samples

Blood was collected from healthy donors (18–64 years old) in endotoxin-free tubes with K3-EDTA (Labor Import, Brazil). All participants gave their written informed consent for blood collection, after being informed of the procedures and after declaring no symptoms of chronic or infectious diseases (cough, fever, fatigue, body pain, etc.), nor stress and alcohol ingestion in the last 24 h before the blood collection. Table S1 summarizes healthy donors' records. The research protocol followed the World Medical Association Declaration of Helsinki and was approved by the Institutional Review Board of the Federal University of Santa Catarina (UFSC, CAAE #82815718.2.0000.0121). Blood samples also were collected from severe COVID-19 patients ($n = 6$; 25 to 89 years old) and convalescent COVID-19 patients ($n = 8$; 25 to 89 years old) admitted to the intensive care unit (ICU) or NUPAIVA (Research Center on Asthma and Airway Inflammation) at the UFSC University Hospital from August to October 2020. Samples from severe COVID-19 patients ($n = 10$; 49 to 93 years old) admitted to the Pneumology Department from Cochin Hospital and critically ill COVID-19 patients ($n = 6$; 49 to 93 years old) in the ICU from Bichat Hospital, Assistance Publique-Hôpitaux de Paris, France (February 2021 to January 2022), were included also. Table S2 summarizes patients' clinical and laboratory records. Blood samples from sex-matched healthy donors were used as controls (Table S1). All patients, donors or a close family member, gave consent for participation in the study, which was approved by the Institutional Review Board of the UFSC (CAAE #36944620.5.1001.0121) and the Comité de Protection des Personnes Nord Ouest IV (ID-RCB 2020-A02700-39).

EDTA-anticoagulated blood was used to isolate neutrophils and monocytes using the Ficoll density gradient centrifugation method (Witko-Sarsat et al., 2010), followed by EasySep™ HLA Chimerism CD15 Positive Selection Kit for neutrophils and StemSep™ Human CD14 Positive Selection Kit for monocytes according to manufacturers' instructions. Then, purified isolated cells (99%) were resuspended in RPMI-1640 medium (Gibco, Thermo Fisher, Waltham, MA, USA) containing 10% fetal bovine serum (FBS) (Thermo Fisher). These samples were used to analyse surface Sia content and cell response.

2.2 | Evaluation of neutrophil response

Experiments were carried out either with 1×10^6 isolated neutrophils or whole blood containing 1×10^6 leukocytes. Cells were incubated (37°C, 5% CO₂) in the presence or absence of LPS ($1 \mu\text{g}\cdot\text{ml}^{-1}$, *Escherichia coli* 0127:b8, Sigma-Aldrich, St. Louis, MO, USA), recombinant human (rh) S100A8 protein ($2 \mu\text{M}$, R&D Systems, Minneapolis, MN, USA), oseltamivir ($100 \mu\text{M}$, Sigma-Aldrich) or zanamivir ($30 \mu\text{M}$, Sigma-Aldrich) for 90 min, preincubated or not with *Maackia amurensis* lectin II (MAL-II) ($1 \mu\text{g}\cdot\text{ml}^{-1}$, Vector Labs, San Diego, CA, USA) or the metalloproteinase 9 inhibitor (MMP-9i) (CAS 1177749-58-4, 5 nM, Calbiochem) for 30 min. The concentrations of oseltamivir

($100 \mu\text{M}$) and zanamivir ($30 \mu\text{M}$) used were chosen by concentration-effect curves ($10\text{--}300 \mu\text{M}$ oseltamivir and $1\text{--}100 \mu\text{M}$ zanamivir) (Figure 1h–m) with minimum effect on cell apoptosis/necrosis (95% of cell viability). The concentrations of oseltamivir and zanamivir used in our in vitro system are similar to the concentrations found in human serum and tissues after drug absorption (Cass et al., 1999; Davies, 2010). To avoid competition between sialylated proteins present in plasma and cell surface, only isolated neutrophils or total leukocytes were used instead of whole blood to evaluate the effect of NEU from *Clostridium perfringens* (CpNEU) on neutrophils. Either isolated neutrophils or total leukocytes were incubated (37°C, 5% CO₂) in the presence or absence of CpNEU (10 mU , Sigma-Aldrich), oseltamivir ($100 \mu\text{M}$) or zanamivir ($30 \mu\text{M}$) for 60 min, after preincubation (30 min) or not with MAL-II ($1 \mu\text{g}\cdot\text{ml}^{-1}$). Thereafter, the following assays were performed.

2.2.1 | Analysis of neutrophil activation

Either isolated neutrophils or total leukocytes were resuspended in flow cytometry (FACS) buffer (2 mM EDTA/PBS). The antibodies anti-CD66b (G10F5; BioLegend), CD62L (DREG-56; BioLegend), CD16 (3G8; BioLegend), CD11b (ICRF44; BioLegend), CXCR2 (5E8; BioLegend) and NEU1 (Proteintech, UK) and the respective isotypes or MAL-II (Vector Labs) coupled to streptavidin (BioLegend), *Sambucus nigra* (elderberry bark) lectin (SNA, Thermo Fisher), peanut agglutinin from *Arachis hypogaea* (PNA, Thermo Fisher) plus human BD Fc Block™ (BD Pharmingen™) and Fixable Viability Stain (FVS, BD Horizon™, San Jose, CA, USA) were added to leukocytes for 30 min at 4°C. Human monocytes were stained with the antibodies anti-CD14 (M0Pg; BD Biosciences), CD11b, CD11c (3.9; BioLegend) or CD64 (10.1; BD Biosciences) and the lectins MAL-II, SNA or PNA. Cells were washed, resuspended in FACS buffer, acquired in a FACSVerser (BD Biosciences, Piscataway, NJ, USA) or Cytex Aurora (Cytex Biosciences, Fremont, CA, USA) cytometer and analysed using FlowJo software (FlowJo LLC). Approximately 100,000 gated events were acquired in each analysis (gate strategy shown in Figure S1).

2.2.2 | Probing cells with Siglec-9-Fc

Siglec-9 ligands were labelled by incubation of chimeric protein containing Siglec-9 Sia-immunoglobulin-binding domain fused to a human IgG-Fc portion (Siglec-9-Fc). Siglec-9-Fc probe was incubated with $\alpha\text{-IgG1-Alexa Fluor 488}$ for 1 h at 4°C prior to adding it into cell culture. Next, cells were incubated with human BD Fc Block™ (30 min, 4°C), washed and stained for 1 h at 4°C with Siglec-9-Fc- $\alpha\text{-IgG1-Alexa Fluor 488}$.

2.2.3 | Phagocytosis assays

After RBC lysis, 1×10^6 leukocytes were incubated at either 37°C (5% CO₂) or 4°C (control) with $100 \mu\text{g}\cdot\text{ml}^{-1}$ pHrodo™ Red *E. coli*

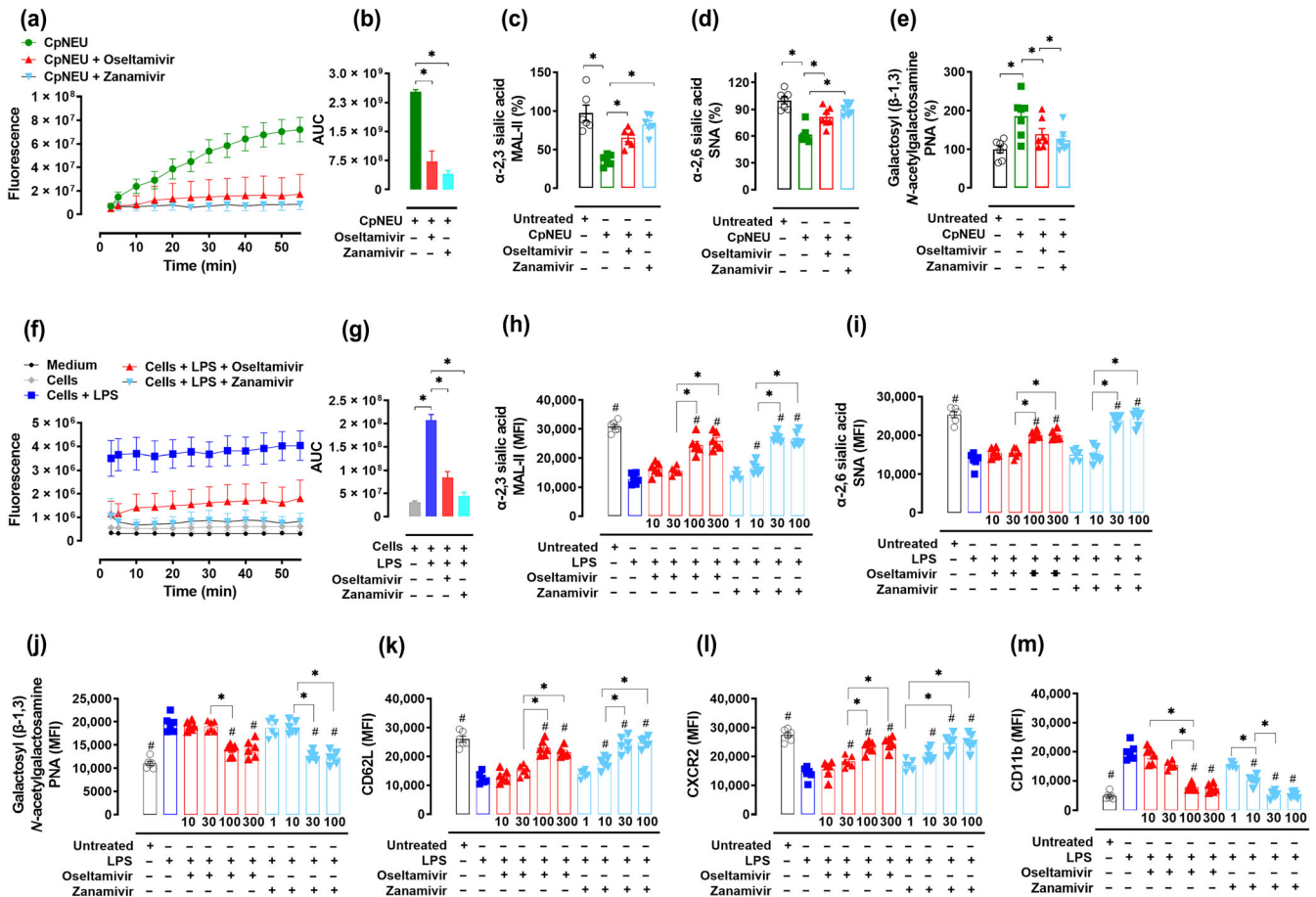


FIGURE 1 Lipopolysaccharide (LPS) stimulates neuraminidase (NEU) activity in human neutrophils. NEU from *Clostridium perfringens* (CpNEU) was used to validate the NEU activity assay. CpNEU (0.012 UI) was added to a 96-well flat-bottom dark plate on ice in the presence or absence of oseltamivir phosphate (100 μ M) or zanamivir (30 μ M). Next, the substrate 4-methylumbelliferyl-N-acetyl- α -D-neuraminic acid (4-MU-NANA) (0.025 mM) was added, and the fluorescent resulting product read at 37°C for 55 min (a). The area under the curve (AUC) values are shown in (b). Isolated neutrophils (1×10^6) from healthy donors ($n = 6$) were stimulated or not with CpNEU (0.012 UI, 60 min, 37°C, 5% CO₂) in the presence or absence of oseltamivir (100 μ M) or zanamivir (30 μ M). Neutrophils were then stained with *Maackia amurensis* lectin II (MAL-II) to detect α -2,3 sialic acids (c), *Sambucus nigra* lectin (SNA) to detect α -2,6 sialic acids (d) or peanut agglutinin (PNA) to detect galactosyl (β -1,3) N-acetylgalactosamine (e) using flow cytometry analysis. Cells (0.5×10^6 ; $n = 5$) resuspended in HBSS were added to a plate on ice, and 4-MU-NANA substrate (0.025 mM) was added followed by the addition of medium and LPS (1 μ g·ml⁻¹, 60 min, 37°C, 5% CO₂) in the presence or absence of oseltamivir (100 μ M) or zanamivir (30 μ M) (f). The AUC values are shown in (g). The property of LPS in stimulating endogenous NEU from human isolated neutrophils ($n = 6$) was evaluated using different concentrations of oseltamivir (10, 30, 100 and 300 μ M) or zanamivir (1, 10, 30 and 100 μ M). Sialic acid content was assessed using staining with MAL-II (h), SNA (i) and PNA (j), and cell activation was evaluated by staining CD62L (k), CXCR2 (l) and CD11b (m) by flow cytometry. The MFI or the percentage (%) in relation to the unstimulated control group was analysed on CD66b⁺/CD15⁺ cells using the gate strategies shown in Figure S1. * $P < 0.05$. #Significantly different compared to LPS-stimulated groups. Symbols represent individual donors, and data are shown as mean \pm SEM from experiments conducted with at least five different individuals.

BioParticles[®] (Thermo Fisher) for 60 min and the MFI of neutrophils (FVS⁻/CD66b⁺ cells) with ingested bioparticles were analysed by FACS. Total leukocytes were incubated with 1×10^6 colony-forming units (CFU) of live *E. coli* (ATCC 25922) for 90 min (37°C, 5% CO₂). Next, the cells were washed twice (2 mM EDTA/PBS) and fixed (FACS buffer/PFA 2%), and the percentage of neutrophils with bacteria or the percentage of neutrophils with ≥ 3 bacteria was analysed by light microscopy using the Differential Quick Stain Kit (Laborclin, Brazil).

2.2.4 | Bacterial killing

Total leukocytes (1×10^6) were incubated (37°C, 5% CO₂) with 1×10^6 CFU of live *E. coli* for 180 min. The samples were centrifuged (270 g, 7 min, 4°C), and 10 μ l of supernatant was diluted until 10^6 and spread onto an agar brain-heart infusion (BHI, Kasvi, Brazil) to quantify the viable extracellular bacteria. The pellets were washed twice with PBS/2 mM EDTA (270 g, 7 min, 4°C); the leukocytes were lysed with 2% Triton X, washed (PBS, 2000 g, 15 min,

4°C) and resuspended in PBS; and 10 μl of samples was diluted until 10^6 and spread onto agar BHI. Plates were incubated overnight at 37°C, and viable bacteria were expressed as mean \pm SEM of CFU. ml^{-1} .

2.2.5 | Analysis of ROS production

Total leukocytes (1×10^6) were incubated at 37°C (5% CO_2) with 10 μM of cell-permeant 2',7'-dichlorodihydrofluorescein diacetate (CM-H2DCFDA, Thermo Fisher) for 5 min. Next, cells were stimulated or not with 0.1 $\mu\text{g}\cdot\text{ml}^{-1}$ phorbol 12-myristate 13-acetate (PMA) for 10 min, fixed, washed twice with PBS/2 mM EDTA (270 g, 7 min, 4°C) and analysed by FACS. Isolated neutrophils (1×10^5) were washed and resuspended with 0.1 ml of HBSS containing 10 μM of the cell-permeant luminol and stimulated with or without PMA (0.1 $\mu\text{g}\cdot\text{ml}^{-1}$), opsonized zymosan (OZ) (0.5 $\mu\text{g}\cdot\text{ml}^{-1}$) or N-formylmethionine-leucyl-phenylalanine (fMLF) peptide (1 μM). Chemiluminescence (CL) was recorded at 37°C in a luminometer (Berthold-Biolumat LB937) in duplicate over 40 min and expressed as integrated total counts.

2.2.6 | NET assay

NET quantification was performed on the supernatant of isolated neutrophils. Briefly, an anti-MPO antibody bound to a 96-well flat-bottom plate captured the enzyme MPO (5 $\mu\text{g}\cdot\text{ml}^{-1}$; Abcam), and the amount of DNA bound to the enzyme was quantified using the Quant-iT™ PicoGreen® kit (Invitrogen, Carlsbad, CA, USA) according to the manufacturer's instructions. Fluorescence intensity (ex 488 nm/em 525 nm) was quantified in a FlexStation 3 Microplate Reader (Molecular Devices, San Jose, CA, USA).

2.3 | NEU kinetic assay

Isolated neutrophils or total leukocytes (0.5×10^6) were resuspended in Hanks' Balanced Salt Solution (HBSS) and added to a 96-well flat-bottom dark plate (SPL Life Sciences, South Korea) on ice. Then, 4-methylumbelliferyl-N-acetyl- α -D-neuraminic acid (4-MU-NANA, Sigma-Aldrich) substrate (0.025 mM) was added followed by medium, or LPS (1 $\mu\text{g}\cdot\text{ml}^{-1}$), rh S100A8 (2 μM), oseltamivir (100 μM), zanamivir (30 μM), MAL-II (1 $\mu\text{g}\cdot\text{ml}^{-1}$) or MMP-9i (5 μM). CpNEU (10 mU) with or without oseltamivir or zanamivir was used as positive controls of the assay. The volume was completed to 200 μl with HBSS, followed by reading on the Spectramax® Paradigm® or Tecan® Fluorescence Microplate Reader, starting 3 min after and every 5 min for 30 or 55 min at 37°C. Sialidase activity was assessed in isolated neutrophils, using heat-inactivated or fresh plasma from severe COVID-19 patients in the presence or absence of oseltamivir (100 μM) or zanamivir (30 μM), using the Tecan

Infinite 200 multi-reader. The fluorescent substrate 4-MU-NANA formation was detected at ex 350 nm/em 450 nm.

2.4 | Immunofluorescence and Duolink proximity ligation assay (PLA)

Isolated neutrophils (0.3×10^6 per slide) were fixed with 2% paraformaldehyde for 30 min and blocked with 5% BSA/PBS. Cells were then incubated for 1 h at 37°C with *M. amurensis* lectin II biotinylated (15 $\mu\text{g}\cdot\text{ml}^{-1}$) or mouse anti-human NEU1 (1:50; Proteintech, UK) diluted in 1% BSA/PBS. After PBS washing, cells were incubated with Streptavidin Alexa Fluor 555 conjugate (1:1000; s32355 Life) or goat anti-mouse secondary antibody coupled to Alexa Fluor 555 (1:500; Thermo Fisher) for 30 min at 37°C. For the Duolink PLA (Sigma-Aldrich) assay, cells were incubated first with both mouse anti-human NEU1 (1:100) and then a rabbit anti-human MMP-9 (1:100; Invitrogen), following the procedures according to the manufacturer's instructions. Slides were prepared and nuclei stained with mounting medium containing DAPI (Sigma-Aldrich). Stained cells were examined with a widefield Zeiss fluorescence microscope (magnification 100 \times), and the images were imported into ImageJ software for analysis. Images were captured from different fields. Immunostaining was assessed as the mean in each field from different donors and normalized by the number of DAPI-positive cells. The Immuno-related procedures used comply with the recommendations made by the *British Journal of Pharmacology*.

2.5 | scRNA-seq analysis

Publicly available single cell RNA-sequencing data (scRNA-Seq), profiling nasopharyngeal or pooled nasopharyngeal/pharyngeal swabs (NSs), bronchial protected specimen brushes (PSBs) and bronchial lavages (BLs), were downloaded from https://figshare.com/articles/COVID-19_severity_correlates_with_airway_epithelium-immune_cell_interactions_identified_by_single-cell_analysis/12436517. Raw count data, normalized data and UMAP coordinates generated by the authors of the original publication were imported into CellRouter for downstream analysis.

2.6 | Neutrophil responses with plasma from COVID-19 patients

Whole-blood samples from sex-matched healthy donors ($n = 7$) were incubated for 2 h (37°C, 5% CO_2) with 7% of fresh plasma from healthy donors, severe or convalescent COVID-19 patients or heat-inactivated plasma (56°C, 30 min) from severe COVID-19 patients in the presence or absence of oseltamivir (100 μM) or zanamivir (30 μM). Surface levels of α -2,3-Sia and CD66b and ROS production were assessed in neutrophils by FACS.

2.7 | Mice

Animal welfare and experimental procedures were carried out strictly in accordance with the Guide for the Care and Use of Laboratory Animals (National Institutes of Health, USA). Animal studies are reported in compliance with the ARRIVE guidelines (Percie du Sert et al., 2020) and with the recommendations made by the *British Journal of Pharmacology* (Lilley et al., 2020). Protocols were approved by the Animal Use Ethics Committee of UFSC (CEUA #8278290818). Male and female C57BL/6 (25–30 g) and Swiss mice (35–40 g) were provided by the Animal Facility from MIP department or by the Central Animal Facility from the Federal University of Santa Catarina, respectively, and used for peritonitis- or pneumonia-induced severe sepsis. C57BL/6 mice provided by the Central Animal House of the Federal University of Minas Gerais were used in the lung injury model induced by the murine coronavirus mouse hepatitis virus 3 (MHV-3) (CEUA #8278290818). Animals were maintained in an environmentally controlled room (20–22°C, 40–60% relative humidity and a 12 h alternating light/dark cycle with free access to water and food). Laboratory animals were randomly assigned to groups of equal size. Analysis of all animal samples was carried out in a blinded manner. All efforts were made to minimize the animals' suffering and to reduce the number of animals used. Animals were euthanized in a CO₂ chamber followed by cervical dislocation if humane endpoints were reached (weight loss ≥20% of pre-experimental body weight).

2.8 | *E. coli*-, *Klebsiella pneumoniae*- and CLP-induced sepsis

E. coli (ATCC 25922, Manassas, VA, USA) or *K. pneumoniae* (ATCC 700603) were used for peritonitis- or pneumonia-induced severe sepsis in mice. Naive mice were intraperitoneally (IP) challenged with 100 µl of 1×10^7 CFU of the *E. coli* suspension. A group of *E. coli*-septic mice was randomly pretreated (2 h before infection) and post-treated *per oral* (PO, 12/12 h) with either saline or oseltamivir phosphate (10 mg·kg⁻¹, Eurofarma, Brazil) for 4 days for survival analysis. Another group was pretreated 2 h before infection with a single dose of oseltamivir phosphate (10 mg·kg⁻¹, PO), and the pathophysiological response was analysed at 4 and 6 h after infection. *E. coli*-septic mice were randomly post-treated (6 h after infection, 12/12 h) with either saline or oseltamivir phosphate (PO, 10 mg·kg⁻¹) for 4 days for survival analysis. For pneumonia-induced sepsis, mice were anaesthetized with isoflurane (3–5 vol%) and placed in supine position. A small incision was made in the neck where the trachea was localized, and a *K. pneumoniae* suspension (4×10^8 CFU/50 µl of PBS) was injected into the trachea with a sterile 30-gauge needle. The skin was sutured, xylazine (5 ml kg⁻¹ IP) given as an analgesic agent, and animals were left for recovery in a warm cage. After 6 h of infection and then 12/12 h, mice were treated with oseltamivir phosphate (PO, 10 mg·kg⁻¹) for survival analysis. In another set of experiments, pneumonia was induced and mice were treated 6 h after infection with a single dose of oseltamivir phosphate (10 mg·kg⁻¹, PO) for material

collection and analysis of the pathophysiological response 24 h after infection. For caecal ligation and puncture (CLP)-induced sepsis model, mice were anaesthetized with xylazine (2 mg·kg⁻¹, IP, Syntec, Brazil) followed by isoflurane (3–5 vol%, BioChimico, Brazil), a 1 cm midline incision was made in the anterior abdomen, and the caecum was exposed and ligated below the ileocaecal junction. The caecum was punctured twice with an 18-gauge needle and gently squeezed to allow its contents to be released through the punctures. Sham-operated (Sham) animals underwent identical laparotomy but without CLP. The caecum was repositioned in the abdomen, and the peritoneal wall was closed. All animals received 1 ml of 0.9% saline subcutaneously (SC) and 100 µl of tramadol (5 mg·kg⁻¹, SC, Vitalis, Brazil) immediately after CLP. CLP-septic mice were randomly treated (starting 6 h after infection, PO) with 100 µl of either saline or oseltamivir phosphate (10 mg·kg⁻¹, 12/12 h) for 36 h. In another set of experiments, CLP mice were randomly IP treated (6 h after infection, 12/12 h) during 4 days with 100 µl metronidazole (15 mg·kg⁻¹, Isofarma, Brazil) plus ceftriaxone (40 mg·kg⁻¹, Eurofarma, Brazil) and oseltamivir phosphate (10 mg·kg⁻¹) or saline by PO for survival analysis, or treated for 36 h to analyse the pathophysiological response at 48 h after CLP.

2.9 | MHV-3-induced acute lung injury

Prior to infection, the MHV-3 strain provided and sequenced (GenBank Accession No. MW620427.1) by Clarice Weis Arns and Ricardo Durães-Carvalho from the State University of Campinas (UNICAMP, Brazil) was propagated in media containing L929 cells (ATCC CCL-1), as previously described (Andrade et al., 2021). Mice (6–7 weeks old) were IP anaesthetized with ketamine (50 mg·kg⁻¹) and xylazine (5 mg·kg⁻¹) and intranasally inoculated with 30 µl of sterile NaCl 0.9% solution, containing or not MHV-3 (3×10^3 plaque-forming units [PFUs]). Then, mice were treated or not orally with oseltamivir phosphate (10 mg·kg⁻¹) diluted in 0.5% sodium carboxymethyl cellulose (v/v) twice a day beginning 24 h after inoculation. On the third day after inoculation, the peak of infection, all animals were euthanized in a CO₂ chamber followed by cervical dislocation to collect lungs for further analysis. Lungs were immediately frozen in liquid nitrogen or fixed with 10% neutral buffered formalin (v/v) solution for histopathological analysis.

2.10 | Neutrophil migration

The animals were euthanized in a CO₂ chamber followed by cervical dislocation, the bronchoalveolar lavage (BAL) and peritoneal lavage (PL) were performed and the number of neutrophils was determined at 4 and 6 h after *E. coli*, 24 h after *K. pneumoniae* infection or 48 h after CLP surgery. Next, mice were perfused with PBS/EDTA (1 mM), and the lungs were harvested. Lungs were passed through 40 µm nylon cell strainers, and single-cell suspensions were centrifuged in 35% Percoll® solution (315 mOsm·kg⁻¹, Sigma-Aldrich) for 15 min at 700 g to enrich leukocyte populations. Pelleted cells were then collected, and

erythrocytes were lysed. Single-cell suspensions from individual mice were determined, either using a cell counter (Coulter ACT, Beckman Coulter, Brea, CA, USA) or with a haemocytometer. Differential counts were determined on Cytospin smears stained using the Differential Quick Stain Kit (Laborclin, Brazil). Blood samples were collected by heart puncture and tubes containing **heparin** for further analysis. Neutrophils from PL or BAL were stained with anti-Ly-6G/Ly-6C (GR-1, RB6-8C5; BioLegend) and MAL-II to be further analysed by FACS, as previously described. Analysis was carried out in SSC^{high}/GR-1^{high} cells.

In mice from the murine betacoronavirus-induced acute lung injury, neutrophil infiltration into the lungs was assessed indirectly by myeloperoxidase (MPO) assay in lung homogenates, as previously described (Cassini-Vieira et al., 2015).

2.11 | Bacterial counts and viral titration

The bacterial counts were determined in the BAL, PL or blood from septic mice by harvesting 10 µl of samples plated on Mueller–Hinton agar dishes (Difco Laboratories, Waltham, MA, USA) and incubated for 24 h at 37°C for determination of CFUs. PL or BAL samples were diluted until 10⁶. Lungs from murine betacoronavirus-infected mice were collected, and 30 mg of tissue from each mouse was used. Tissues were homogenized in 300 µl of DMEM (7% FBS) and centrifuged (2000 g; 5 min), and supernatants were collected. Prior to that, in a 24 well-plate, L929 cells (1.5 × 10⁵ per well) were seeded and grown to confluence. Cell layers were incubated with 0.1 ml of the serially diluted supernatants for 1 h and overlaid with 1.6% methylcellulose + DMEM with 2% FBS. Plates were incubated for 2 days at 37°C, fixed in 10% formaldehyde and stained with 1% crystal violet in water for 30 min for PFU counting.

2.12 | ELISA

TNF (R&D Systems, Minneapolis, MN, USA) and **IL-17** (XpressBio Life Sciences Products, Frederick, MD, USA) levels in plasma, PL or BAL were determined by ELISA kits according to the manufacturers' instructions.

2.13 | Tissue injury biochemical markers

Aspartate aminotransferase (AST), alanine aminotransferase (ALT) and alkaline phosphatase (ALP) activities and the levels of total **bilirubin** were determined in plasma samples derived from the employed sepsis models using commercial kits (Labtest Diagnóstica, Brazil). The procedures were carried out according to the manufacturer's instructions.

2.14 | Histopathological liver analysis

Formalin-fixed and paraffin-embedded lung tissues from murine betacoronavirus-infected mice were sectioned into 5-µm-thick slices

and stained with haematoxylin and eosin (H&E). A total of two sections for each animal were examined, and results were plotted as the mean of damage values in each mouse. Image acquisition and analysis were performed using an Olympus BX microscope (Olympus). The histopathological evaluation was conducted by a pathologist in a blinded manner, using a scoring system encompassing airway inflammation (up to 4 points), vascular inflammation (up to 4 points), parenchyma inflammation (up to 5 points) and general neutrophil infiltration (up to 5 points), as previously described (Andrade et al., 2021).

2.15 | Statistical analysis

The data were obtained from three to seven independent experiments using at least n = 5 for human samples. We used five mice per experimental group, except for survival analyses in which 12 to 20 mice were used. The mean or median values for the different groups were compared by analysis of variance (ANOVA) followed by Dunnett and/or Tukey post-tests. Bacterial counts were analysed by the Mann–Whitney *U*-test or unpaired *t* test using a parametric test with Welch's correction. Survival curves were plotted using the Kaplan–Meier method and then compared using the log-rank method and Gehan–Wilcoxon test. Data were analysed using GraphPad Prism Version 8.00 for Mac (GraphPad Software, USA). A *P* < 0.05 was considered significant. The data and statistical analysis comply with the recommendations of the *British Journal of Pharmacology* on experimental design and analysis in pharmacology (Curtis et al., 2018).

2.16 | Materials

Details of materials and suppliers are provided in the specific subsections in Methods

2.17 | Nomenclature of targets and ligands

Key protein targets and ligands in this article are hyperlinked to corresponding entries in <http://www.guidetopharmacology.org> and are permanently archived in the Concise Guide to PHARMACOLOGY 2021/22 (Alexander et al., 2021).

3 | RESULTS

3.1 | LPS-induced surface Sia shedding and human neutrophil activation is mediated by NEU activity

The neutrophil response *in vivo* involves a complex network of multiple cell types and soluble mediators. Therefore, using whole blood as an *in vitro* system to study neutrophil activation provides a closer

physiological environment for cells when compared with experiments using isolated cells (Duffy et al., 2014; Messerer et al., 2020). Because neutrophil activation could lead to NEU activity and consequently hydrolyse Sia residues on the cell surface (Varki, 2008), we evaluated Sia levels on neutrophils after LPS activation. LPS treatment of whole blood from healthy donors significantly reduces the binding of the lectin *M. amurensis* II (MAL-II, binds selectively for α -2,3-linked Sia over α -2,6-linked Sia) (Knibbs et al., 1991) on neutrophils when compared with untreated cells (Figure S2A). Next, cells were stained with an Fc-chimera of Siglec-9, which is a Sia-binding protein that recognizes Sia in α -2,3 and α -2,6 linkages (Movsisyan & Macauley, 2020). The binding of Siglec-9-Fc (Figure S2B) was decreased on neutrophils treated with LPS, confirming a reduction of neutrophil Sia residues likely due to LPS-induced NEU activity in these cells. To test this hypothesis, we measured NEU activity in human leukocytes using the NEU substrate 4-MU-NANA (Amith et al., 2009) and validated the assay using CpNEU. We used total

leukocytes instead of whole blood, because plasmatic factors could lead to an overestimation of cellular NEU activity. Both clinically available NEU inhibitors, oseltamivir and zanamivir, reduced CpNEU activity (Figure 1a,b). Moreover, these NEU inhibitors decreased CpNEU-mediated reduction of the lectins MAL-II (Figure 1c) or *S. nigra* (SNA) binding (SNA, binds selectively to α -2,6-linked Sia over α -2,3-linked Sia) (Figure 1d), as well as the binding of peanut agglutinin (PNA, binds to non-sialylated galactose residues (Varki & Gagneux, 2012) on neutrophils (Figure 1e). LPS-induced NEU activity on leukocytes was significantly inhibited by oseltamivir or zanamivir (Figure 1f,g). We also analysed the surface expression of CD66b and CD62L, two markers of human neutrophil activation (Jutilla et al., 1989; Schmidt et al., 2012), as well as α -2,3-Sia levels in LPS-exposed whole-blood cultures. Both NEU inhibitors constrained the shedding of Sia (Figure S3A–C) and CD62L (Figure S4A,B), or the up-regulation of CD66b (Figure S4C,D). Next, we evaluated the effect of LPS-induced surface Sia shedding and cell activation in isolated cells

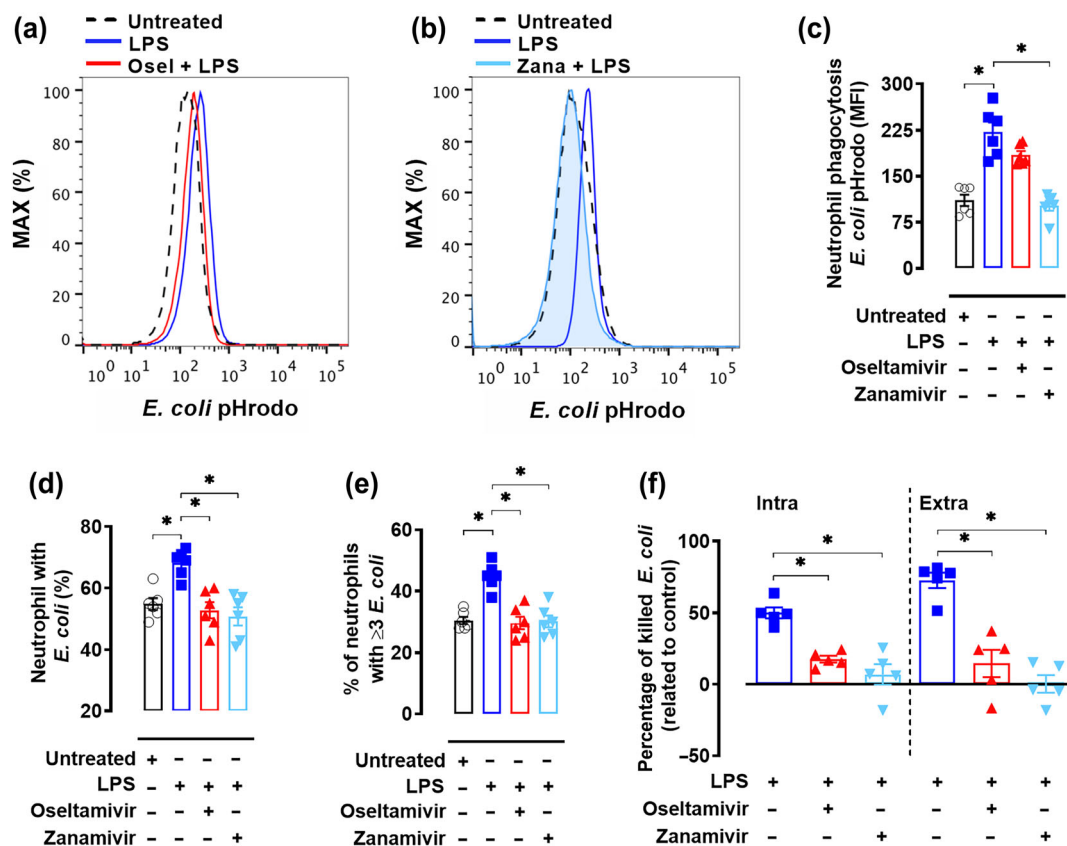


FIGURE 2 Lipopolysaccharide (LPS) increases phagocytosis and killing of *E. coli* in a NEU-dependent manner. Whole blood from healthy donors ($n = 6$) containing 1×10^6 leukocytes was incubated or not with LPS ($1 \mu\text{g}\cdot\text{ml}^{-1}$, 90 min, 37°C , 5% CO_2) in the presence or absence of oseltamivir ($100 \mu\text{M}$) or zanamivir ($30 \mu\text{M}$). The *E. coli* pHrodo BioParticles[®] ($100 \mu\text{g}\cdot\text{ml}^{-1}$) were used for 60 min at 37°C to assess phagocytosis by flow cytometry. Representative histograms were used to show the effect of oseltamivir (a) and zanamivir (b) or by the MFI (c) in viable $\text{CD}66\text{b}^+/\text{CD}15^+$ cells (as gated in Figure S1). Live *E. coli* was used to assess phagocytosis by light microscopy or to investigate bacterial killing by leukocytes. Cells were stimulated as described above, and 1×10^6 leukocytes were incubated at 37°C with *E. coli* (1×10^6 colony-forming units [CFU]) for 90 min for phagocytosis ($n = 6$) or for 180 min for the killing assay ($n = 5$). The percentage of cells with ingested bacteria (d) and the number of bacterial particles per cell (e, ≥ 3 particles per cell) were evaluated. The killing of *E. coli* was studied by spreading $10 \mu\text{l}$ of supernatant (extracellular killing) or $10 \mu\text{l}$ of the intracellular or membrane adhered content in agar medium for CFU counting. The killing was expressed as the rate of fold change compared to the unprimed (untreated) cells (f). Symbols represent individual donors, and data are shown as mean \pm SEM from experiments conducted with at least five different individuals. $P < 0.05$

(neutrophils or monocytes). Similar to whole-blood experiments, incubation of isolated neutrophils with either oseltamivir or zanamivir reduced LPS-induced surface Sia shedding and cell activation in a dose-dependent manner (Figure 1h–m). Moreover, a similar pattern response was observed using isolated monocytes (Figure S5A–G). Together, these results show that LPS-induced host NEU activity decreases Sia content and activates neutrophils, which can be inhibited by oseltamivir and zanamivir.

3.2 | LPS-induced neutrophil response is modulated by NEU activity

The uptake and killing of bacteria are important functions of neutrophils (Alves-Filho et al., 2010). We next investigated whether host NEU regulates phagocytosis and killing of *E. coli*. Whole blood from healthy donors was preincubated (90 min) with LPS and *E. coli* Bio-Particles[®] added to cells for 60 min. Ingested pHrodo *E. coli* by neutrophils were analysed by flow cytometry. A significant increase in the MFI of unstimulated cells incubated with pHrodo *E. coli* was observed at 37°C compared to cells at 4°C (Figure S6). Oseltamivir or zanamivir significantly inhibited the LPS-increased phagocytosis (Figure 2a–c). Similarly, pretreatment of cells with LPS increased both the number of cells with bacteria and number of bacteria per cell (Figure 2d,e). In agreement, LPS enhanced membrane expression of phagocytic receptors CD11b in isolated neutrophils (Figure 1m) and CD11b/CD11c in isolated monocytes (Figure S5D,E). These effects were decreased when NEU inhibitors oseltamivir and zanamivir were added in the cell cultures (Figures 1m, 2d,e and S5D,E). LPS treatment also enhanced intracellular and extracellular killing of *E. coli*, which was inhibited by oseltamivir or zanamivir (Figure 2f). When we primed the cells with CpNEU as a positive control of NEU outcomes, we observed effects similar to those seen with LPS on phagocytosis and killing of *E. coli* (Figure S7A–F). These results suggest that NEU plays a critical role in LPS-up-regulated phagocytosis and killing responses of neutrophils.

Next, we assessed whether NEU inhibitors influenced LPS-stimulated ROS production and release of NETs, which are key mediators of bacterial killing and tissue injury (Mittal et al., 2014). Whole-blood neutrophils primed with LPS and stimulated with PMA produced higher amounts of ROS when compared with unstimulated cells (Figure S8A–C). Both oseltamivir and zanamivir inhibited ROS release to levels similar to unstimulated cells. Furthermore, oseltamivir or zanamivir significantly inhibited LPS-induced NETs released by isolated neutrophils (Figure S8D). Accordingly, isolated neutrophils stimulated with the recombinant human S100A8 (rh S100A8) protein, a toll-like receptor (TLR) 4 agonist (Vogl et al., 2018), showed similar effects of LPS by inducing host NEU activity (Figure S9A,B), shedding of surface Sia levels (Figure S9C–E), cell activation (Figure S9F,G) and ROS production (Figure S9H). In the presence of oseltamivir and zanamivir, the effects of rh S100A8 were inhibited. These findings strengthened the concept that TLR4-induced neutrophil activation involves NEU activity.

3.3 | NEU1–MMP-9 interaction is involved on LPS-induced human neutrophil activation

To understand how NEU is activated in neutrophils, we evaluated the expression of NEU1, because this isoform was found to regulate cellular responses through engagement with membrane receptors (Amith et al., 2009). We observed that NEU1 is expressed at low levels on the surface of unstimulated human neutrophils (Figure 3a) and its expression increased after LPS challenge (Figure 3a–c). Next, we investigated the interaction of MMP-9 with NEU1, because their crosstalk seems to be essential for TLR signalling on other cell types (Abdulkhalek et al., 2011). Using the Duolink[®] PLA assay, we observed that LPS increased surface NEU1–MMP-9 interplay (Figure 3d,e). Then, we used the selective MMP-9 inhibitor (MMP-9i) to investigate the dependence of this molecule in inducing NEU activity. Preincubation of isolated neutrophils with MMP-9i prevented NEU activity (Figure 3f,g) as well as preventing the shedding of surface Sia and the neutrophil response (Figure 3h–n). These findings suggested that MMP-9 activity was essential for NEU1 activation on human neutrophils. Next, we preincubated cells with MAL-II as a tool to prevent the hydrolysis of α -2,3-Sia, because this lectin can block the NEU cleavage site (Amith et al., 2010). Preincubation of isolated neutrophils with MAL-II did not inhibit LPS-induced NEU activity (Figure 3f,g), but prevented the shedding of surface Sia (Figure 3h–j) and neutrophil activation (Figure 3k–n). The effect of oseltamivir, zanamivir, MAL-II or MMP-9i on ROS production was evaluated on isolated neutrophils stimulated with LPS plus PMA, OZ or fMLF. All assessed drugs were able to inhibit ROS production on cells stimulated with LPS plus PMA or OZ, but not on cells stimulated with fMLF (Figure 4a–i), suggesting a non-promiscuous role for NEU activation in this effect. Together, these data showed that dampening NEU activity by oseltamivir, zanamivir or MMP-9i or blocking the hydrolysis of α -2,3-Sia was sufficient to inhibit human neutrophil response induced by LPS.

3.4 | Oseltamivir enhances the survival rate of mice in clinically relevant models of sepsis

Exacerbated neutrophil responses, such as increased ROS production, the release of NET and degranulation, are associated with tissue injury and organ dysfunction (Sônego et al., 2016). By using oseltamivir as a therapeutic tool, we next explored the involvement of NEU activity in vivo during experimental sepsis, a model of neutrophil dysfunction (Alves-Filho et al., 2010; Spiller et al., 2010, 2012). We first induced sepsis by IP administration of 1×10^7 CFU per mice of the Gram-negative *E. coli* (ATCC 25922), which lacks NEU in its genome (Vimr & Troy, 1985). We used a dose of $10 \text{ mg} \cdot \text{kg}^{-1}$ of oseltamivir by oral gavage, which is the equivalent dose used in humans ($\sim 7.5 \text{ mg} \cdot \text{kg}^{-1}$) (Butler et al., 2020). Oseltamivir pretreatment (2 h before infection) plus post-treatment (6 h after infection, 12/12 h, PO, for 4 days) markedly boost host survival (Figure S10A). Only a single dose of oseltamivir 2 h before bacterial administration significantly

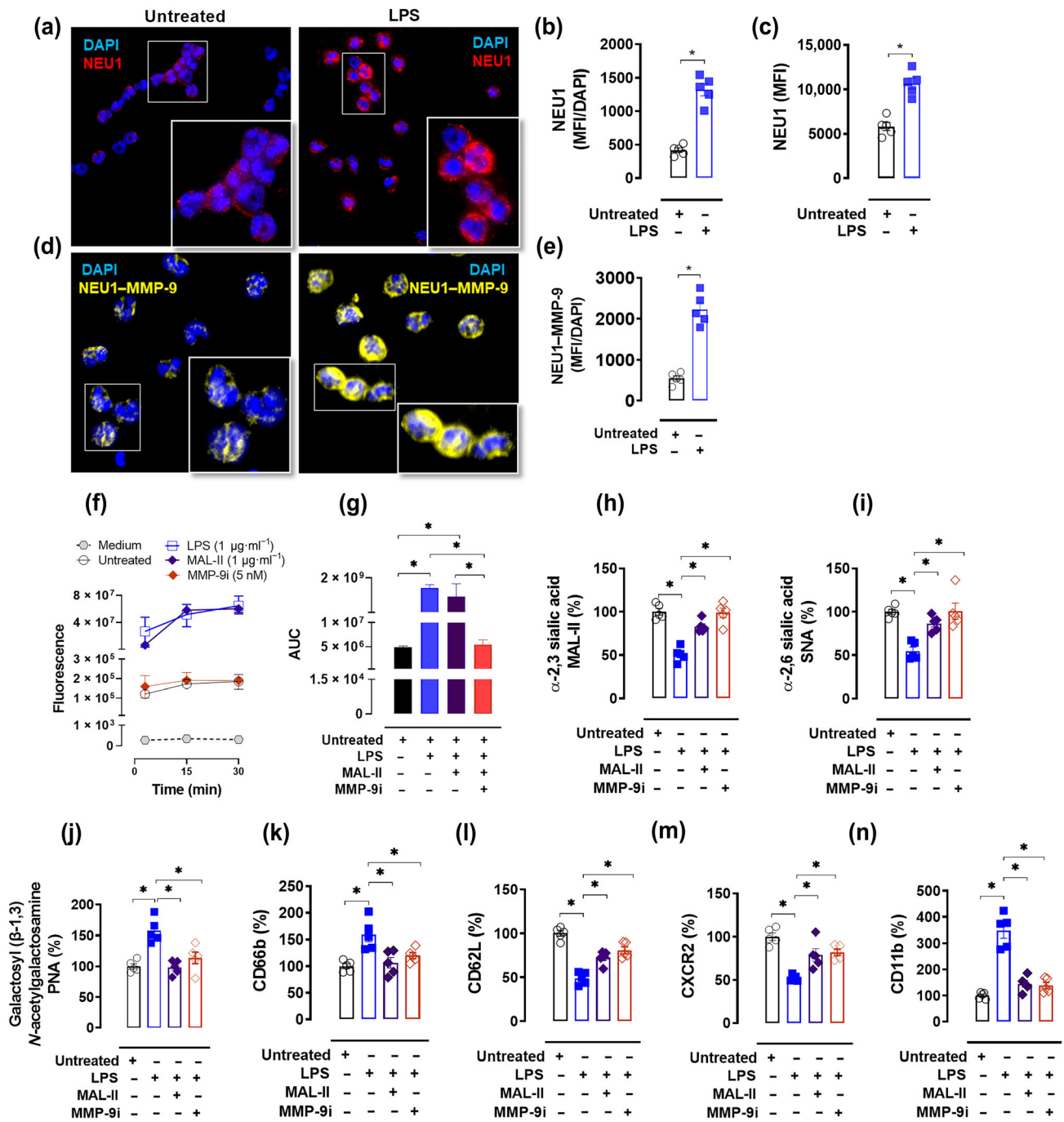


FIGURE 3 Legend on next page.

FIGURE 3 Lipopolysaccharide (LPS)-induced NEU1 activity is dependent on matrix metalloproteinase 9 (MMP-9) in human neutrophils. Isolated neutrophils from healthy donors ($n = 5$) were stimulated or not with LPS ($1 \mu\text{g}\cdot\text{ml}^{-1}$, 90 min, 37°C , 5% CO_2), and cytospin slides containing 0.3×10^6 cells were used to detect NEU1 membrane staining (red) and 4',6-diamidino-2-phenylindole (DAPI) for the fluorescent deoxyribonucleic acid (DNA) stain (blue) by indirect immunofluorescence (a). A similar approach was carried out showing NEU1 in the membrane of isolated neutrophils (1×10^6) by FACS (c). NEU1–MMP-9 surface interaction (yellow) was assessed using the Duolink[®] proximity ligation assay (PLA) (d). Merged representative photos (magnification 100 \times) were captured from at least three different fields and analysed using ImageJ[®] 1.53J software. MFI was assessed in each captured field (each point corresponds to the mean of a different donor) and normalised by the number of DAPI-positive cells (b, e). LPS-stimulated neutrophils (1×10^6 , $n = 5$) in the presence or absence of *Maackia amurensis* lectin II (MAL-II) ($1 \mu\text{g}\cdot\text{ml}^{-1}$, MAL-II promotes steric hindrance at the NEU cleavage site and prevents sialic acid cleavage) or the selective MMP-9 inhibitor (5 nM) was added 30 min prior to LPS incubation. Neutrophil-derived neuraminidase activity was assessed using 4-methylumbelliferyl-N-acetyl- α -D-neuraminic acid (4-MU-NANA) substrate (f). The area under the curve (AUC) values are shown in (g). Cells ($n = 5$) were also then stained in the conditions described above with MAL-II to detect α -2,3 sialic acids (h), *Sambucus nigra* lectin (SNA) to detect α -2,6 sialic acids (i) or peanut agglutinin (PNA) to detect galactosyl (β -1,3) N-acetylgalactosamine (j). The cell activation markers CD66b (k), CD62L (l), CXCR2 (m) and CD11b (n) were evaluated by flow cytometry. The percentage (%) in relation to the unstimulated group was analysed on CD66b⁺/CD15⁺ cells using the gate strategies shown in Figure S1. $^*P < 0.05$. Symbols represent individual donors, and data are shown as mean \pm SEM from experiments conducted with at least five different individuals.

decreased the number of neutrophils in the BAL and lung tissue 4 or 6 h after infection (Figure S10B,C). This pretreatment augmented neutrophil migration to the focus of infection, which was associated with a more efficient infection control (Figure S10D–F). Furthermore, pretreatment with oseltamivir decreased BAL and plasma TNF and IL-17 levels (Figure S10G–J) and decreased tissue injury markers (AST, ALT, ALP and total bilirubin) (Figure S10K–N), as well as preventing reduction of α -2,3-Sia on PL SSC^{high}/GR-1^{high} cells (Figure S10O,P). More importantly, the post-treatment efficacy of oseltamivir was evaluated in survival of septic mice. Mice were IP challenged with *E. coli* (1×10^7 CFU per mice) and treated 6 h after infection with oseltamivir for 4 days ($10 \text{ mg}\cdot\text{kg}^{-1}$, PO, 12/12 h). Strikingly, in the post-treatment protocol, oseltamivir provided a significant improvement in the survival rate of septic mice (Figure S10Q).

Next, we employed the CLP model to evaluate the effect of oseltamivir in septic mice, because it is considered the gold standard in preclinical sepsis (Rittirsch et al., 2009). Six hours after CLP, oseltamivir post-treatment led to a small delay in the mortality rate of severe septic mice (Figure S11A). Next, CLP-septic mice were treated with antibiotics because it is one of the standard interventions used in clinical settings of sepsis (Rhodes et al., 2017). Importantly, compared to the control animals, the therapeutic use of oseltamivir plus antibiotics drastically improved survival rates of CLP mice (87.5% experimental group vs. 25% control group) (Figure S11B). Forty-eight hours after surgery, post-treated septic mice had a significant reduction of neutrophils in BAL and lungs, improvement of neutrophil migration at the focus of infection and reduced bacterial load in PL and blood (Figure S11C–G). Levels of TNF and IL-17 in PL and plasma and tissue injury markers were reduced in oseltamivir-treated mice (Figure S11H–O). Additionally, oseltamivir led to a higher expression of α -2,3-Sia on SSC^{high}/GR-1^{high} cells in PL (Figure S11P,Q) confirming blockade of NEU activity in vivo.

Since respiratory tract infections, particularly during pneumonia, are among the most common sites of infection in sepsis (Chou et al., 2020), we intratracheally administered *K. pneumoniae* (ATCC 700603) to mice to address the effect of oseltamivir. Post-treatment of mice with oseltamivir significantly improved survival of septic mice

challenged with *K. pneumoniae* (Figure 5a). The increased host survival was accompanied by a decrease of neutrophil migration in BAL, reduced levels of TNF and IL-17 and reduced levels of tissue injury markers (Figure 5b–k). Oseltamivir also prevented the reduction of α -2,3-Sia on BAL SSC^{high}/GR-1^{high} cells (Figure 5l,m). Together, these results showed that host NEU activation exacerbated inflammatory responses during sepsis and the use of oseltamivir improves disease outcomes.

3.5 | NEU inhibition rescues overactivated neutrophils from severe COVID-19 patients and decreased lung damage in MHV-3-infected mice

Similar to bacterial sepsis, recent evidence suggests that neutrophils fuel a hyper-inflammatory response during severe SARS-CoV-2 infection. Larger numbers of circulating neutrophils have been associated with poor prognosis of COVID-19 patients, and analysis of lung biopsies and autopsy specimens showed extensive neutrophil infiltration (Kuri-Cervantes et al., 2020; Veras et al., 2020; Wilk et al., 2020). Further studies employing single-cell RNA sequencing (scRNA-seq) from upper and lower respiratory tract samples from COVID-19 patients indicated a significant augmentation of neutrophils linked to a transcriptional programme associated with tissue damage in epithelial and immune cells (Chua et al., 2020). Re-analysis of scRNA-seq data showed that expression of NEU1, but not NEU3 or NEU4, is up-regulated in resident cells and highly expressed in neutrophils found in nasopharyngeal/pharyngeal swabs from COVID-19 patients (Figure 6). A similar profile of NEU expression was observed in lower respiratory tract samples from these patients (Figure S12). These results suggest that NEU1 expressed by lung infiltrating neutrophils may play an important role during cell-induced tissue damage in severe COVID-19. As previously demonstrated, circulating neutrophils are highly activated in active, but not convalescent, COVID-19 patients (Schulte-Schrepping et al., 2020), as observed by CD62L shedding (Figure 7a,j) and up-regulation of CD66b (Figure 7b,k). Moreover, neutrophils from severe COVID-19 patients were found to

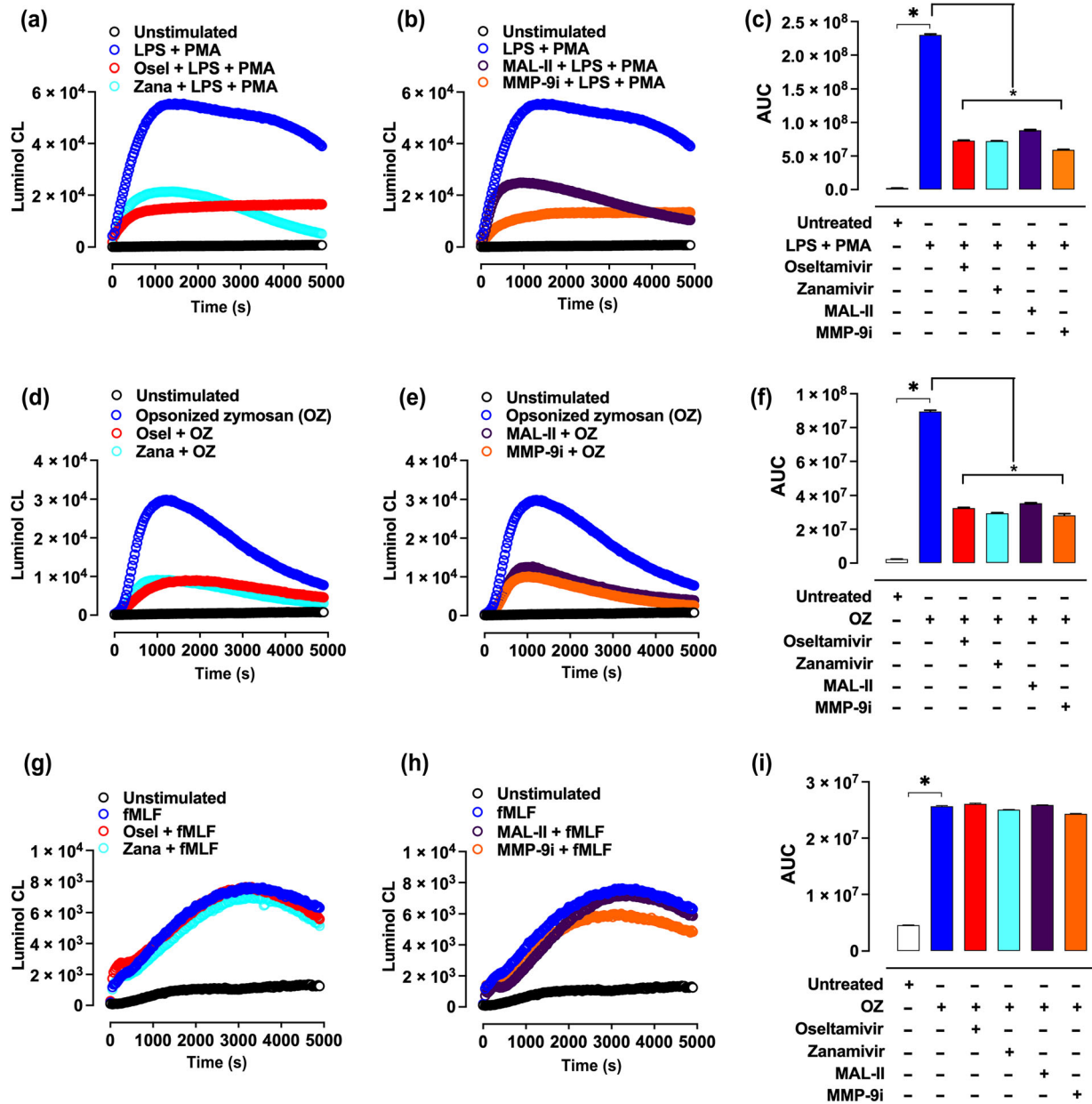


FIGURE 4 Lipopolysaccharide (LPS)- or opsonized zymosan-induced ROS production by human neutrophils is dependent on NEU/matrix metalloproteinase 9 (MMP-9) activity. Isolated neutrophils (1×10^6) from healthy donors ($n = 5$) were stimulated or not with LPS ($1 \mu\text{g}\cdot\text{ml}^{-1}$, 90 min, 37°C , 5% CO_2) in the presence or absence of oseltamivir ($100 \mu\text{M}$) or zanamivir ($30 \mu\text{M}$). Experiments also were conducted using pretreatment with *Maackia amurensis* lectin II (MAL-II) ($1 \mu\text{g}\cdot\text{ml}^{-1}$) or the selective MMP-9 inhibitor (5 nM) added 30 min prior to LPS incubation. Cells were washed and resuspended in HBSS containing luminol and stimulated or not with phorbol 12-myristate 13-acetate (PMA) ($0.1 \mu\text{g}\cdot\text{ml}^{-1}$), opsonized zymosan (OZ; $0.5 \mu\text{g}\cdot\text{ml}^{-1}$) or *N*-formylmethionine-leucyl-phenylalanine (fMLF) ($1 \mu\text{M}$) for chemiluminescence (CL) detection. Kinetic analysis of luminol CL was expressed as integrated total counts for oseltamivir and zanamivir (a, d, g) or followed the pretreatment with MAL-II or MMP-9i (b, e, h). The area under the curve (AUC) values are shown in (c), (f) and (i). * $P < 0.05$. Data are shown as mean \pm SEM from experiments performed in duplicates with five different healthy donors ($n = 5$).

present a significant reduction of surface α -2,3-Sia (Figure 7c,f,g). Likewise, NEU activity was increased in blood neutrophils in both critical ICU and severe COVID-19 patients when compared to healthy controls (Figure 7d,e). In agreement with the scRNA-seq data (Figures 6 and S12), NEU1 was found to be up-regulated on the surface of circulating neutrophils from severe COVID-19 patients compared with cells from healthy controls (Figure 7h,i).

Because soluble NEU enzymes are present in plasma (Yang et al., 2018), we next asked if plasma from COVID-19 patients can induce the neutrophil response in healthy donors. Indeed, stimulation of whole blood from healthy donors with fresh plasma from severe, but not convalescent, COVID-19 patients led to neutrophil activation (Figure 7p), a reduction of α -2,3-Sia (Figure 7q) as well as ROS production (Figure 7r), which were significantly inhibited by oseltamivir or

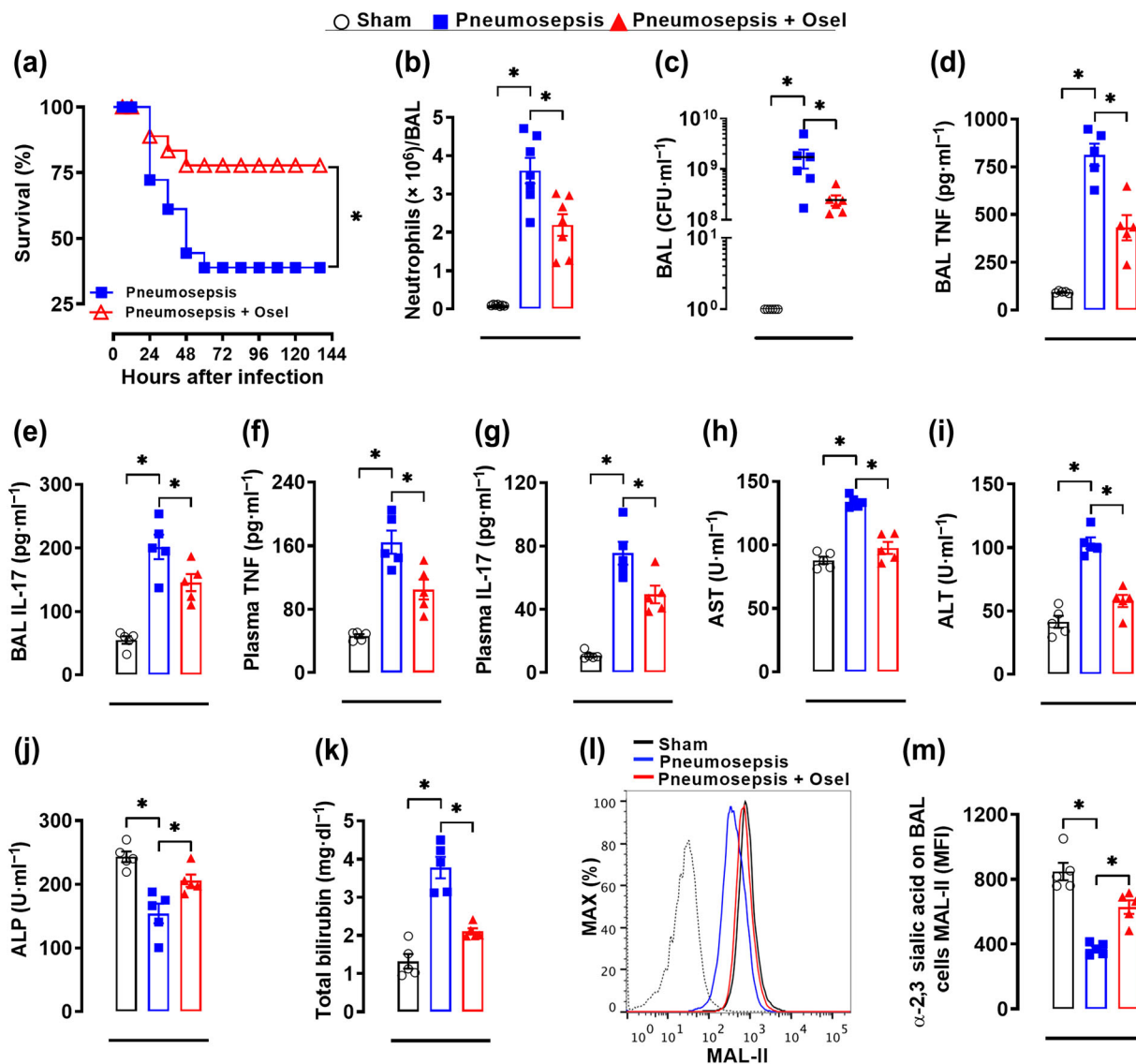


FIGURE 5 Osetamivir (Osel) enhanced mice survival in *Klebsiella pneumoniae*-induced sepsis. Sepsis was induced by intratracheal administration of *K. pneumoniae*, and mice were randomly treated (starting 6 h after infection, 12/12 h, PO, $n = 20$) with saline or Osel phosphate ($10 \text{ mg}\cdot\text{kg}^{-1}$), and survival rates were monitored for 144 h (a). In a similar set of experiments, septic mice ($n = 5$) were treated 6 h after infection with a single dose of Osel phosphate ($10 \text{ mg}\cdot\text{kg}^{-1}$, PO), and mice were euthanized 24 h after infection to determine the number of neutrophils (b), colony-forming units (CFUs) (c) and the levels of TNF (d) and IL-17 (e) in bronchoalveolar lavage (BAL). Plasma levels of TNF (f), IL-17 (g), aspartate aminotransferase (AST) (h), alanine aminotransferase (ALT) (i), alkaline phosphatase (ALP) (j) and total bilirubin (k) were evaluated 24 h after infection. The amount of surface α -2,3 sialic acids was assessed by *Maackia amurensis* lectin II (MAL-II) staining in SSC^{high}/GR-1^{high} cells in BAL and analysed by FACS, as shown by the representative histograms (l) and MFI (m); dotted line = unstained cells. The results are expressed as percent of survival, mean or median (only for FACS data) \pm SEM. * $P < 0.05$. Sham, sham-operated mice

zanamivir (Figure 7p-r). Additionally, NEU activity was increased in fresh plasma from severe COVID-19 patients (Figure S13A). However, plasma samples from severe COVID-19 patients that were heat inactivated to inhibit soluble NEU activity (Figure S13B) still induced neutrophil activation (Figure 7p-r), suggesting that cellular NEU in conjunction with other circulating factors mediates NEU-dependent neutrophil activation in severe COVID-19.

Finally, we addressed the effect of NEU inhibition in an in vivo model of acute lung injury induced by intranasal administration of the murine betacoronavirus MHV-3. As previously described, this model

led to local inflammatory response, tissue damage and impairment of lung functions followed by systemic manifestations, which resembled many characteristics of severe COVID-19 disease (Andrade et al., 2021). The osetamivir post-treatment of infected mice significantly decreased viral load (Figure 8a) and reduced neutrophil infiltration into the lungs (Figure 8b). Histological analysis of pulmonary tissue revealed that osetamivir decreased the inflammatory infiltrate in the perivascular and peribronchiolar region related to a significant lower histopathological score (Figure 8c,d), which indicated protection of lung architecture.

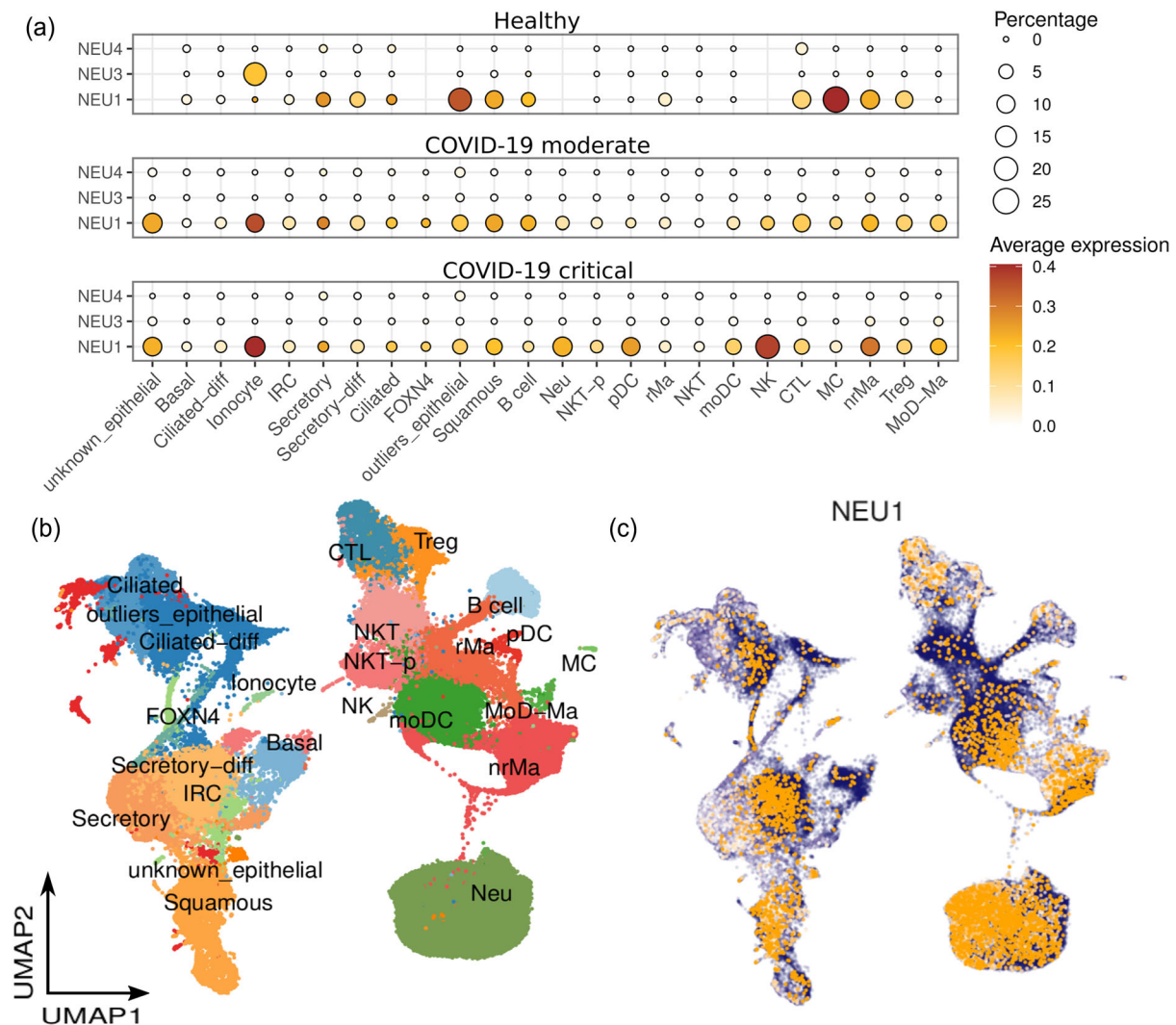


FIGURE 6 High expression of NEU1 in cell types from COVID-19 patients. Gene expression of NEU1, NEU3 and NEU4 across cell types in healthy donors, moderate or critical COVID-19 patients. The size of the circle is proportional to the percentage of cells expressing the reported genes at a normalized expression level higher than one (a). UMAP analysis colour coded by cell types in nasopharyngeal/pharyngeal swab samples from healthy donors and COVID-19 patients (b). Normalized expression of NEU1 overlaid on the UMAP spaces (c).

4 | DISCUSSION

Systemic inflammatory responses may lead to unsuitable neutrophil stimulation, which is associated with higher mortality rates in sepsis and sepsis-like diseases (Leliefeld et al., 2016). Therefore, finding new therapeutic targets to prevent neutrophil overstimulation while maintaining their microbicidal abilities is greatly needed. Based on the findings presented here, NEU inhibitors are promising drugs to fill this gap. We demonstrated that endogenous NEU mediated exacerbated inflammatory responses by stimulated primary neutrophils.

All four different isotypes of NEU described in mammals (NEU1, NEU2, NEU3 and NEU4) remove Sia from glycoproteins and glycolipids with specific substrate preferences (Smutova et al., 2014). NEU1 preferentially cleaves α 2-3-Sia and seems to be the most important isoenzyme in immune cells. NEU1 is a lysosomal enzyme but also is present on the cell surface where it can regulate multiple

receptors, such as Fc gamma receptor (Fc γ R), [insulin receptor](#), [integrin \$\beta\$ -4](#) and [TLRs](#) (Glanz et al., 2019). Although several stimuli were described to induce NEU activity, including LPS (Amith et al., 2009), PMA, calcium ionophore A23187 (Cross & Wright, 1991) and IL-8 (Cross et al., 2003), how the enzyme is activated is poorly understood. However, NEU1 activation involves the formation of a multi-complex of enzymes that stabilize NEU1 in its conformational active state (Pshezhetsky & Hinek, 2011) and where NEU1 was found to be associated with MMP-9 at the surface of naive macrophages (Abdulkhalek et al., 2011). LPS binding to TLR4 leads to the activation of a G protein-coupled receptor (GPCR) via the G α i subunit and MMP-9 to induce NEU1 activity, which in turn removes α 2,3-Sia from TLR4, allowing its dimerization and intracellular signalling (Abdulkhalek et al., 2011; Amith et al., 2010; Feng et al., 2012). We observed a similar phenomenon in human neutrophils, where LPS induced NEU1 translocation to the cell surface and increased its

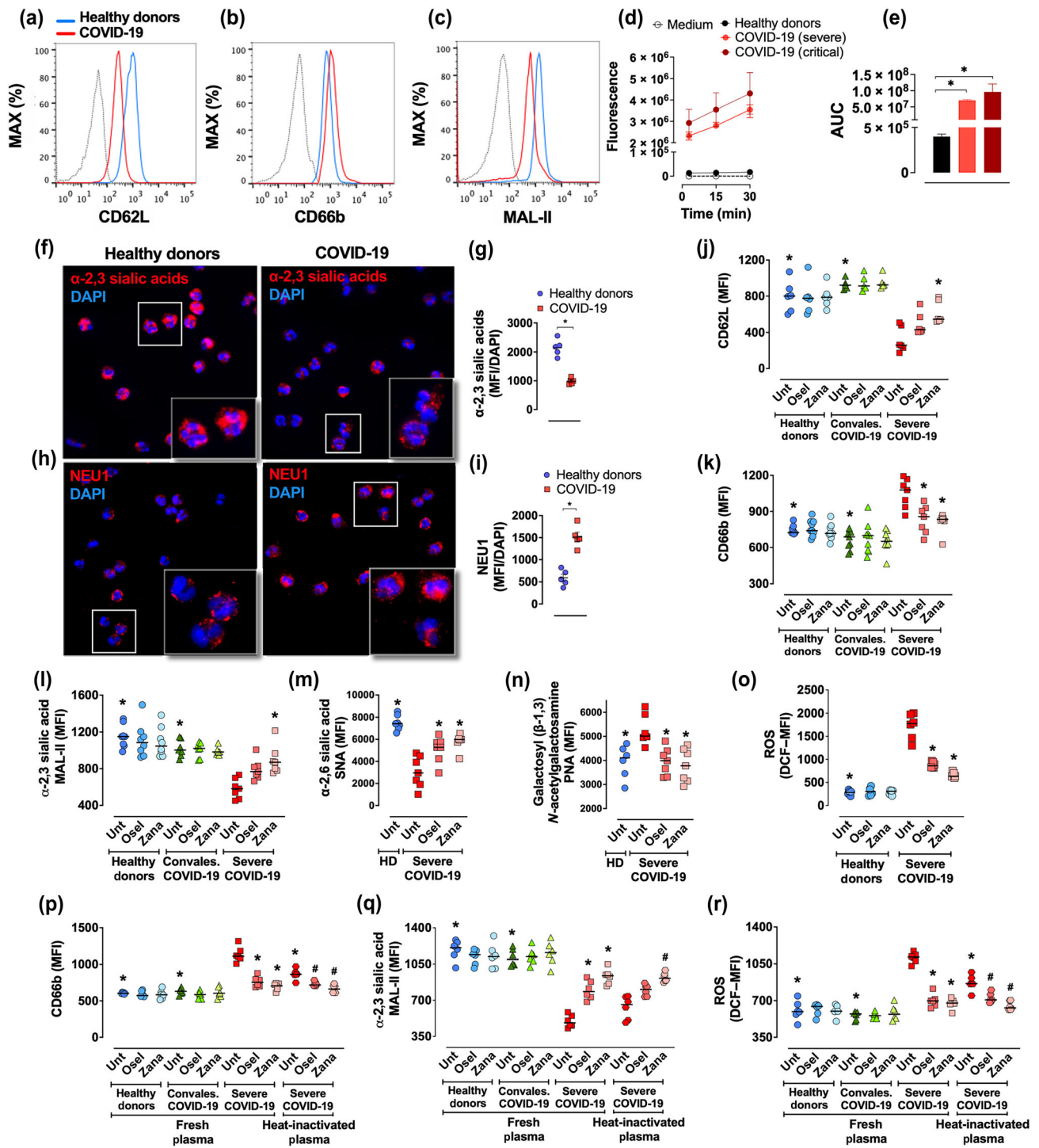


FIGURE 7 Legend on next page.

FIGURE 7 Oseltamivir (Osel) and zanamivir (Zana) decrease neutrophil activation and increase sialic acid levels in active, but not convalescent neutrophils from COVID-19 patients. Whole blood from healthy donors and severe, critical ICU or convalescent COVID-19 patients was treated or not with Osel (100 μ M) or Zana (30 μ M), and total leukocytes were stained with the cell activation markers CD62L (a, j), CD66b (b, k) or the lectins *Maackia amurensis* lectin II (MAL-II) (c, f, l), *Sambucus nigra* lectin (SNA) (m) and peanut agglutinin (PNA) (n) ($n = 6-7$ per group). Isolated neutrophils (0.5×10^6) from healthy controls ($n = 5$) and severe ($n = 6$) or critical ICU COVID-19 patients ($n = 5$) were added in a 96-well flat-bottom dark plate on ice. Next, the substrate 4-MU-NANA (0.025 mM) was added, and the resulting fluorescent product read at 37°C for 30 min (d). The area under the curve (AUC) values are shown in (e). Cytospin slides containing 0.3×10^6 unstimulated neutrophils from healthy donors ($n = 5$) or severe COVID-19 patients ($n = 5$) were used to detect α -2,3 sialic acids (f) or NEU1 (h) membrane staining (red) as well as 4',6-diamidino-2-phenylindole (DAPI) for the fluorescent deoxyribonucleic acid (DNA) stain (blue) by indirect immunofluorescence. Representative images (1000 \times) were captured from at least three different fields and analysed using ImageJ 1.53J software. MFI was assessed in each captured field (each point corresponds to the mean of a different donor) and normalized by the number of DAPI-positive cells (g, i). Total reactive oxygen species (ROS) production was assessed by FACS in isolated neutrophils at the basal state from healthy donors ($n = 6$) or severe COVID-19 patients ($n = 6$) using the CM-H2DCFDA probe (o). Total blood from healthy donors ($n = 7$) was incubated (2 h, 37°C, 5% CO₂) with 7% fresh plasma obtained from healthy controls and severe or convalescent COVID-19 patients. Incubations were carried out in the presence or absence of 7% of heat-inactivated plasma from severe COVID-19 patients under pretreatment or not with Osel (100 μ M) or Zana (30 μ M). Levels of CD66b (p), surface α -2,3-Sia (MAL-II) (q) and ROS production (r) were assessed by FACS. The MFI was analysed on CD66b⁺/CD15⁺ cells using the gate strategies shown in Figure S1. Symbols represent individual donors, and data are shown as scatter dot plots with lines at median from pooled data of two to seven independent experiments. The accepted level of significance for the test was $P < 0.05$. *Significantly different when compared with untreated severe COVID-19. #Significantly different when compared with untreated heat-inactivated plasma from severe COVID-19

association with MMP-9. Interestingly, inhibition of MMP-9 reduced NEU activity, shedding of surface α -2,3-Sia, cell activation and ROS production. Thus, it is possible that NEU1-MMP-9 crosstalk controls Sia levels in TLR4 molecules in human neutrophils, as observed in macrophages and dendritic cells (Amith et al., 2010; Feng et al., 2012). The upstream involvement of NEU regulating LPS responses by neutrophils agrees with the previous demonstration that TLRs stimulate these cells independent of gene transcription (Blander & Medzhitov, 2004). Together, our data suggested that NEU activation provides a fast response to enhance microbial-induced neutrophil functions. Thus, we speculate that this action could be an evolutionary mechanism by which neutrophils quickly mobilize their microbicidal mediators against pathogens.

Sia removal from the surface of neutrophils markedly changes their adhesiveness, chemotaxis and migration (Cross et al., 2003; Feng et al., 2011; Sakarya, 2004). Despite the fact that we did not address the effect of oseltamivir directly on neutrophils, we observed that in peritonitis- or pneumonia-induced sepsis in mice, oseltamivir prevented the massive neutrophil infiltration into bronchoalveolar spaces or lung tissues, suggesting that regulation of neutrophil migration by dampening NEU activity contributes to the survival of septic mice. Interestingly, we observed a divergent effect of oseltamivir on neutrophil migration to the focus of infection between peritonitis- and pneumonia-induced sepsis. This effect could be explained by the different mechanisms involved in neutrophil migration to the peritoneal cavity and lungs. Although expression of CD62L and rolling of neutrophils to endothelium is necessary for its migration to the peritoneal cavity, it does not seem to be required for migration into the lungs (Alves-Filho et al., 2010; Petri et al., 2008). Moreover, systemic neutrophil activation leads to cell stiffening, resulting in the retention of neutrophils in the small capillaries of the lungs (Worthen et al., 1989), which is frequently the first organ impaired in non-pneumonia- and pneumonia-induced sepsis (Sheu et al., 2010).

The role of NEU-induced neutrophil activation suggested here agrees with the previous demonstration that NEU1 deletion in haematopoietic cells confers resistance to endotoxemia (Chen et al., 2018). Also, the sialidase inhibitor Neu5Gc2en protects endotoxemic irradiated wild-type (WT) mice reconstituted with WT bone marrow but not WT mice reconstituted with NEU1^{-/-} bone marrow cells (Chen et al., 2018). Similar to our findings, the treatment of mice with NEU inhibitors increases host survival in *E. coli*-induced sepsis (Yang et al., 2018). This outcome was correlated with significant inhibition of blood NEU activity. Enhancement of soluble NEU activity in serum decreases the Sia residues from ALP enzymes, which are involved in the clearance of circulating LPS phosphate during sepsis (Yang et al., 2018). Therefore, the treatment of mice with NEU inhibitors seems to lead to a systemic inhibition of NEU that is broadly distributed throughout the organism.

SARS-CoV-2 infection in non-vaccinated individuals leads to mild illness in most of the patients, but ~20% of them progress to severe disease with many characteristics resembling sepsis, including acute respiratory distress syndrome (ARDS), cytokine storm and neutrophil dysregulation (Guan et al., 2020; Wang et al., 2020). The transcriptional programmes found in neutrophil subsets from blood and lungs of severe COVID-19 patients are related to cell dysfunction, coagulation and NET formation (Schulte-Schrepping et al., 2020; Silvin et al., 2020; Veras et al., 2020). We observed that blood neutrophils from severe COVID-19 are highly activated, as demonstrated by reduced CD62L expression and increase of CD66b expression, as previously reported (Schulte-Schrepping et al., 2020). We now add new information by showing that NEU1 is highly expressed in both peripheral and infiltrated respiratory tract neutrophils of moderate, severe and critical, but not convalescent, COVID-19 patients. Also, blood neutrophils present reduced surface levels of α -2,3-Sia and α -2,6-Sia, suggesting a relevant role of NEU in COVID-19 pathology. More importantly, both the NEU inhibitors oseltamivir and zanamivir

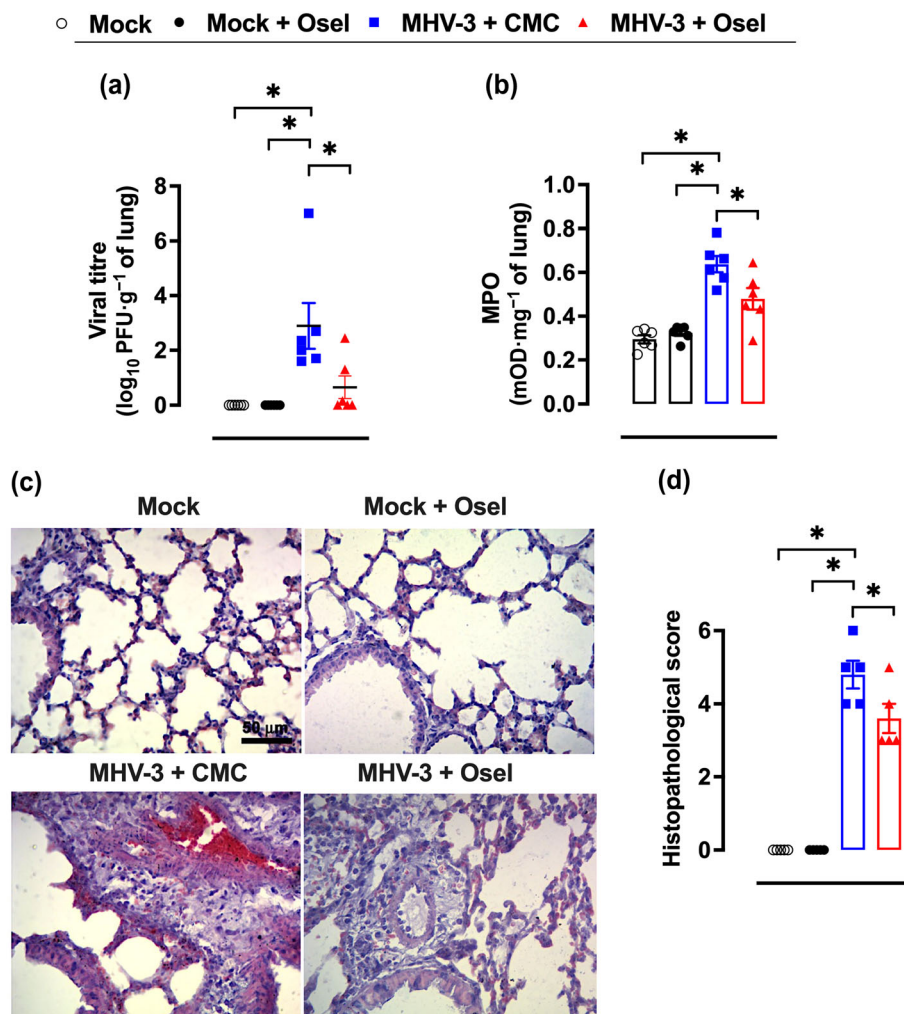


FIGURE 8 Oseltamivir (Osel) treatment inhibits mouse hepatitis virus 3 (MHV-3) replication and inflammation-associated injury in the lungs of wild-type MHV-3-infected mice. C57BL/6 mice ($n = 6$) infection was carried out under anaesthesia with ketamine ($50 \text{ mg}\cdot\text{kg}^{-1}$) and xylazine ($5 \text{ mg}\cdot\text{kg}^{-1}$) by intranasal inoculation with culture medium (mock) or the murine coronavirus MHV-3 (3×10^3 plaque-forming unit [PFU]). After 24 h of inoculation, mice were treated or not with Osel phosphate ($10 \text{ mg}\cdot\text{kg}^{-1}$) or 0.5% sodium carboxymethyl cellulose (CMC) (v/v) starting 24 h after infection, 12/12 h, PO. Three days after infection, all animals were euthanized, and lungs were collected for further analysis. Viral load was assessed in lung lysates by plaque assay, and results were expressed as \log_{10} PFU \cdot g $^{-1}$ of lung tissue (a). Neutrophil infiltration into the lungs was determined indirectly by myeloperoxidase (MPO) activity using a colorimetric assay, and results were expressed as mean optical density (mOD) \cdot mg $^{-1}$ of lungs (b). Histological lung analysis was done using tissues stained with haematoxylin and eosin (H&E), and results were expressed by representative images ($40\times$ magnification; scale: $50 \mu\text{m}$) from the different groups (c) and by a histopathological score analysis (d). The results are expressed as mean \pm SEM. * $P < 0.05$

increased the Sia content and rewired the overactivation of neutrophils in severe COVID-19 patients. We speculate that the addition of NEU competitive inhibitors allowed the endogenous sialyltransferases to restore sialyl residues on surface glycoconjugates. Fast changes in surface Sia levels by sialidases and sialyltransferases seem to be an important mechanism to control neutrophil response (Rifat et al., 2008). Interestingly, the treatment of neutrophils with either oseltamivir or zanamivir also restored the surface levels of CD62L. Despite CD62L shedding being a well-studied phenomenon, the recycling of this molecule is poorly understood. Our results suggested that CD62L could be restored in a fast way and seems to be a beneficial evolutionary mechanism in a cell with a short half-life. In THP-1 cells,

CD62L is in at least two different pools, one at the plasma membrane and one in intracellular vesicles, which can be transported to the surface via TGN network (Dib et al., 2017). We observed an intracellular pool of CD62L in human neutrophils (Figure S14); therefore, it is possible that this CD62L intracellular pool was mobilized to the cell surface during the treatment with NEU inhibitors. In neutrophils from healthy donors or COVID-19 convalescent patients, oseltamivir and zanamivir did not interfere in the resting state and had no effect on Sia content, suggesting that NEU has a low effect on surface Sia turnover on non-activated neutrophils.

How neutrophils are activated and the role of NEU in this process remains to be defined in COVID-19; nevertheless, recent evidence

showed that neutrophils could be directly activated by SARS-CoV-2 (Veras et al., 2020), cytokines (Wang et al., 2020) and alarmins, such as the S100A8/A9 complex (Silvin et al., 2020), a TLR4 ligand (Vogl et al., 2018). Serum S100A8/A9 elevated levels seem to mediate the appearance of overactivated neutrophil subsets and also are implicated in the prediction of severity as well as poor clinical outcome in COVID-19 (Chen et al., 2020; Guo et al., 2021). We now suggest that soluble NEU along with other circulating factors present in plasma accounts for neutrophil activation in COVID-19.

The therapeutic use of NEU inhibitors for COVID-19, such as oseltamivir, has been addressed along the pandemics, and the clinical outcomes associated with treatment seem to be contradictory. Tan et al. (2020) showed that the clinical use of oseltamivir did not improve the patients' symptoms and did not slow disease progression. On the other hand, Liu et al. (2020) conducted a large cohort study in Wuhan (China), pointing out that oseltamivir treatment was beneficial in COVID-19 and associated with a decreased risk of death in severe patients. Some studies also suggest how disease progression and outcome may be improved in combination therapy with oseltamivir (Chiba, 2021; Liu et al., 2020; Tan et al., 2021). Interestingly, we correlate our human in vitro data with the effect of oseltamivir in vivo by showing that treatment of betacoronavirus-infected mice reduced the viral load and decreased neutrophil infiltration into the lungs, consequently ameliorating tissue damage. However, for the establishment of this therapy, further studies will be necessary, and the off-label use of oseltamivir should be conducted carefully and under medical supervision.

Collectively, this work indicates that host NEU1 activation via engagement with MMP-9 leads to the shedding of surface Sia with consequent neutrophil overstimulation. On the other hand, NEU inhibitors prevented shedding of Sia and regulate neutrophil response, resulting in infection control and high survival rates. These findings highlight the role of those enzymes as key regulators of neutrophil functions and suggest this pathway as a potential host-directed intervention to rewire neutrophil responses during systemic inflammation.

ACKNOWLEDGEMENTS

We are grateful for the Universidade Federal de Santa Catarina (UFSC), the Laboratório Multiusuário de Estudos em Biologia (LAMEB/UFSC), Institut Cochin (Université de Paris), Le programme de bourses d'excellence Eiffel (Campus France—Ministère de l'Europe et des Affaires étrangères), CAPES/PrInt (UFSC/Université Paris-Saclay) and CNPq for the institutional, technical and financial support.

AUTHOR CONTRIBUTIONS

Rodrigo de Oliveira Formiga: Conceptualization; data curation; formal analysis; investigation; methodology; writing-original draft; writing-review and editing. **Flávia C. Cardoso:** Conceptualization; investigation. **Camila F. Souza:** Investigation; methodology. **Daniel A. G. B Mendes:** Investigation; methodology. **Carlos WS Wanderley:** Investigation; methodology. **Cristina B. Lorenzini:** Investigation; methodology. **Adara A. Santos:** Investigation; methodology. **Juliana Antônia:**

Investigation; methodology. **Lucas F. Faria:** Investigation; methodology. **Caio C. Natale:** Investigation; methodology. **Nicholas M. Paula:** Investigation; methodology. **Priscila C. S. Silva:** Investigation; methodology. **Fernanda R. Fonseca:** Investigation; methodology. **Luan Aires:** Investigation; methodology. **Nicoli Heck:** Investigation; methodology. **Márick R. Starick:** Formal analysis; investigation; methodology. **Celso M Queiroz-Junior:** Formal analysis; investigation; methodology. **Felipe R.S Santos:** Formal analysis; investigation; methodology. **Filipe R.O de Souza:** Formal analysis; investigation; methodology. **Vivian V Costa:** Conceptualization; formal analysis; investigation; methodology; resources. **Shana P. C. Barroso:** Investigation; methodology. **Alexandre Morrot:** Investigation; methodology; resources. **Johan Van Weyenbergh:** Formal analysis; investigation; methodology; resources. **Regina Sordi:** Investigation; methodology; resources. **Frederico Alisson-Silva:** Investigation; methodology; resources. **Fernando Cunha:** Investigation; methodology; resources. **Edroaldo L. Rocha:** Formal analysis; investigation; methodology; resources. **Sylvie Chollet-Martin:** Formal analysis; investigation; methodology. **Maria Margarita Hurtado-Nedelec:** Formal analysis; investigation; methodology; resources. **Clémence Martin:** Formal analysis; investigation; methodology. **Pierre-Régis Burgel:** Formal analysis; investigation; methodology. **Daniel S. Mansur:** Funding acquisition; investigation; methodology; resources; supervision; writing-original draft. **Rosemeri Maurici:** Investigation; methodology; resources. **Matthew S. Macauley:** Investigation; methodology; resources. **André Báfica:** Conceptualization; funding acquisition; resources; supervision; writing-original draft; writing-review and editing. **Véronique Witko-Sarsat:** Conceptualization; project administration; resources; supervision; writing-original draft; writing-review and editing. **Fernando Spiller:** Conceptualization; formal analysis; funding acquisition; investigation; methodology; project administration; resources; supervision; writing-original draft; writing-review and editing.

AFFILIATIONS

¹Department of Pharmacology, Federal University of Santa Catarina, Florianópolis, Brazil

²Université de Paris, Institut Cochin, INSERM U1016, CNRS, Paris, France

³Laboratory of Immunobiology, Department of Microbiology, Immunology and Parasitology, Federal University of Santa Catarina, Florianópolis, Brazil

⁴Department of Pharmacology, School of Medicine of Ribeirão Preto, University of São Paulo, Ribeirão Preto, Brazil

⁵Department of Clinical Medicine, Federal University of Santa Catarina, Florianópolis, Brazil

⁶Department of Morphology, Institute of Biological Sciences, Federal University of Minas Gerais, Belo Horizonte, Brazil

⁷Department of Biochemistry and Immunology, Institute of Biological Sciences, Federal University of Minas Gerais, Belo Horizonte, Brazil

⁸Molecular Biology Laboratory, Institute of Biomedical Research, Marcilio Dias Naval Hospital, Navy of Brazil, Rio de Janeiro, Brazil

⁹Tuberculosis Research Laboratory, Faculty of Medicine, Federal University of Rio de Janeiro, Rio de Janeiro, Brazil

¹⁰Immunoparasitology Laboratory, Oswaldo Cruz Foundation (FIOCRUZ), Rio de Janeiro, Brazil

¹¹Department of Microbiology, Immunology and Transplantation, Rega Institute for Medical Research, Laboratory for Clinical and Epidemiological Virology, KU Leuven, Leuven, Belgium

¹²Department of Immunology, Paulo de Goes Institute of Microbiology, Federal University of Rio de Janeiro, Rio de Janeiro, Brazil

¹³INSERM UMR 996, 'Inflammation, Microbiome and Immunosurveillance', Faculty of Pharmacy, Université Paris-Saclay, Châtenay-Malabry, France

¹⁴INSERM-U1149, Faculté de Médecine, Site Xavier Bichat, CNRS, Université de Paris, Paris, France

¹⁵Department of Pneumology, AP-HP, Hôpital Cochin, Paris, France

¹⁶Department of Chemistry, Department of Medical Microbiology and Immunology, University of Alberta, Edmonton, Alberta, Canada

CONFLICTS OF INTEREST

The authors declare that no conflicts of interest exist.

DECLARATION OF TRANSPARENCY AND SCIENTIFIC RIGOUR

This Declaration acknowledges that this paper adheres to the principles for transparent reporting and scientific rigour of preclinical research as stated in the *BJP* guidelines for [Design & Analysis](#), [Immunoblotting and Immunochemistry](#), and [Animal Experimentation](#) and as recommended by funding agencies, publishers and other organizations engaged with supporting research.

DATA AVAILABILITY STATEMENT

The authors confirm that the data supporting the findings of this study are available within the article and supporting information. The data that support the findings of this study are available from the corresponding author upon reasonable request. Some data may not be made available because of privacy or ethical restrictions.

ORCID

Rodrigo de Oliveira Formiga  <https://orcid.org/0000-0001-5475-0067>

Felipe R. S. Santos  <https://orcid.org/0000-0002-8392-1467>

Fernando Q. Cunha  <https://orcid.org/0000-0003-4755-1670>

REFERENCES

- Abdulkhalek, S., Amith, S. R., Franchuk, S. L., Jayanth, P., Guo, M., Finlay, T., Gilmour, A., Guzzo, C., Gee, K., Beyaert, R., & Szewczuk, M. R. (2011). Neu1 sialidase and matrix metalloproteinase-9 cross-talk is essential for toll-like receptor activation and cellular signaling. *Journal of Biological Chemistry*, 286(42), 36532–36549. <https://doi.org/10.1074/jbc.M111.237578>
- Alexander, S. P., Cosentino, B. J., Schooley, R. L., Mathie, A., Peters, J. A., Veale, E. L., Armstrong, J. F., Faccenda, E., Harding, S. D., Pawson, A. J., Southan, C., Davies, J. A., Annett, S., Boison, D., Burns, K. E., Dessauer, C., Gertsch, J., Helsby, N. A., Izzo, A. A., ... Wong, S. S. (2021). The Concise Guide to PHARMACOLOGY 2021/22: Enzymes. *British Journal of Pharmacology*, 178(Suppl 1), S313–S411. <https://doi.org/10.1111/bph.15542>
- Alves-Filho, J. C., Spiller, F., & Cunha, F. Q. (2010). Neutrophil paralysis in sepsis. *Shock*, 34, 15–21. <https://doi.org/10.1097/SHK.0b013e3181e7e61b>
- Amith, S. R., Jayanth, P., Franchuk, S., Finlay, T., Seyrantepe, V., Beyaert, R., Pshezhetsky, A. V., & Szewczuk, M. R. (2010). Neu1 desialylation of sialyl α -2,3-linked β -galactosyl residues of TOLL-like receptor 4 is essential for receptor activation and cellular signaling. *Cellular Signaling*, 22, 314–324. <https://doi.org/10.1016/j.cellsig.2009.09.038>
- Amith, S. R., Jayanth, P., Franchuk, S., Siddiqui, S., Seyrantepe, V., Gee, K., Basta, S., Beyaert, R., Pshezhetsky, A. V., & Szewczuk, M. R. (2009). Dependence of pathogen molecule-induced toll-like receptor activation and cell function on Neu1 sialidase. *Glycoconjugate Journal*, 26, 1197–1212. <https://doi.org/10.1007/s10719-009-9239-8>
- Andrade, A. C. D. S. P., Campolina-Silva, G. H., Queiroz-Junior, C. M., de Oliveira, L. C., Lacerda, L. S. B., Gaggino, J. C. P., de Souza, F. R. O., de Meira Chaves, I., Passos, I. B., Teixeira, D. C., Bittencourt-Silva, P. G., Valadão, P. A. C., Rossi-Oliveira, L., Antunes, M. M., Figueiredo, A. F. A., Wnuk, N. T., Temerozo, J. R., Ferreira, A. C., Cramer, A., ... Costa, V. V. (2021). A biosafety level 2 mouse model for studying betacoronavirus-induced acute lung damage and systemic manifestations. *Journal of Virology*, 95(22), e0127621. <https://doi.org/10.1128/JVI.01276-21>
- Arora, D. J. S., & Henrichon, M. (1994). Superoxide anion production in influenza protein-activated NADPH oxidase of human polymorphonuclear leukocytes. *The Journal of Infectious Diseases*, 169, 1129–1133. <https://doi.org/10.1093/infdis/169.5.1129>
- Blander, J. M., & Medzhitov, R. (2004). Regulation of phagosome maturation by signals from toll-like receptors. *Science*, 304, 1014–1018. <https://doi.org/10.1126/science.1096158>
- Butler, C. C., van der Velden, A. W., Bongard, E., Saville, B. R., Holmes, J., Coenen, S., Cook, J., Francis, N. A., Lewis, R. J., Godycki-Cwirko, M., Llor, C., Chlabicz, S., Lionis, C., Seifert, B., Sundvall, P. D., Colliers, A., Aabenhus, R., Bjerrum, L., Jonassen Harbin, N., ... Verheij, T. J. (2020). Oseltamivir plus usual care versus usual care for influenza-like illness in primary care: An open-label, pragmatic, randomised controlled trial. *The Lancet*, 395, 42–52. [https://doi.org/10.1016/S0140-6736\(19\)32982-4](https://doi.org/10.1016/S0140-6736(19)32982-4)
- Cass, L. M., Efthymiopoulos, C., & Bye, A. (1999). Pharmacokinetics of zanamivir after intravenous, oral, inhaled or intranasal administration to healthy volunteers. *Clinical Pharmacokinetics*, 36(Suppl 1), 1–11.
- Cassini-Vieira, P., Moreira, C. F., da Silva, M. F., & da Silva Barcelos, L. (2015). Estimation of wound tissue neutrophil and macrophage accumulation by measuring myeloperoxidase (MPO) and N-acetyl- β -D-glucosaminidase (NAG) activities. *Bioprotocols*, 5, e1662.
- Chang, Y.-C., Uchiyama, S., Varki, A., & Nizet, V. (2012). Leukocyte inflammatory responses provoked by pneumococcal sialidase. *MBio*, 3, e00220–e00211.
- Chen, G.-Y., Brown, N. K., Wu, W., Khedri, Z., Yu, H., Chen, X., van de Vlekkert, D., D'Azzo, A., Zheng, P., & Liu, Y. (2014). Broad and direct interaction between TLR and Siglec families of pattern recognition receptors and its regulation by Neu1. *eLife*, 3, e04066. <https://doi.org/10.7554/eLife.04066>
- Chen, L., Long, X., Xu, Q., Tan, J., Wang, G., Cao, Y., Wei, J., Luo, H., Zhu, H., Huang, L., Meng, F., Huang, L., Wang, N., Zhou, X., Zhao, L., Chen, X., Mao, Z., Chen, C., Li, Z., ... Zhou, J. (2020). Elevated serum levels of S100A8/A9 and HMGB1 at hospital admission are correlated with inferior clinical outcomes in COVID-19 patients. *Cellular & Molecular Immunology*, 17(9), 992–994. <https://doi.org/10.1038/s41423-020-0492-x>
- Chiba, S. (2021). Effect of early oseltamivir on outpatients without hypoxia with suspected COVID-19. *Wiener Klinische Wochenschrift*, 133(7–8), 292–297.

- Chou, E. H., Mann, S., Hsu, T.-C., Hsu, W.-T., Liu, C. C.-Y., Bhakta, T., Hassani, D. M., & Lee, C. C. (2020). Incidence, trends, and outcomes of infection sites among hospitalizations of sepsis: A nationwide study. *PLoS ONE*, 15(1), e0227752. <https://doi.org/10.1371/journal.pone.0227752>
- Chua, R. L., Lukassen, S., Trump, S., Hennig, B. P., Wendisch, D., Pott, F., Debnath, O., Thümann, L., Kurth, F., Völker, M. T., Kazmierski, J., Timmermann, B., Twardziok, S., Schneider, S., Machleidt, F., Müller-Redetzky, H., Maier, M., Krannich, A., Schmidt, S., ... Eils, R. (2020). COVID-19 severity correlates with airway epithelium-immune cell interactions identified by single-cell analysis. *Nature Biotechnology*, 38(8), 970–979. <https://doi.org/10.1038/s41587-020-0602-4>
- Cross, A. S., Sakarya, S., Rifat, S., Held, T. K., Drysdale, B.-E., Grange, P. A., Cassels, F. J., Wang, L. X., Stamos, N., Farese, A., Casey, D., Powell, J., Bhattacharjee, A. K., Kleinberg, M., & Goldblum, S. E. (2003). Recruitment of murine neutrophils in vivo through endogenous sialidase activity. *Journal of Biological Chemistry*, 278(6), 4112–4120. <https://doi.org/10.1074/jbc.M207591200>
- Cross, A. S., & Wright, D. G. (1991). Mobilization of sialidase from intracellular stores to the surface of human neutrophils and its role in stimulated adhesion responses of these cells. *Journal of Clinical Investigation*, 88, 2067–2076. <https://doi.org/10.1172/JCI115536>
- Curtis, M., Alexander, S., Cirino, G., Docherty, J., George, C., Giembycz, M., Hoyer, D., Insel, P., Izzo, A., Ji, Y., MacEwan, D., Sobey, C., Stanford, S., Teixeira, M., Wonnacott, S., & Ahluwalia, A. (2018). Experimental design and analysis and their reporting II: Updated and simplified guidance for authors and peer reviewers. *British Journal of Pharmacology*, 175(7), 987–993. <https://doi.org/10.1111/BPH.14153>
- Davies, B. E. (2010). Pharmacokinetics of oseltamivir: An oral antiviral for the treatment and prophylaxis of influenza in diverse populations. *Journal of Antimicrobial Chemotherapy*, 65(Suppl 2), ii5–ii10. <https://doi.org/10.1093/jac/dkq015>
- Dib, K., Tikhonova, I. G., Ivetic, A., & Schu, P. (2017). The cytoplasmic tail of L-selectin interacts with the adaptor-protein complex AP-1 subunit μ 1A via a novel basic binding motif. *Journal of Biological Chemistry*, 292, 6703–6714. <https://doi.org/10.1074/jbc.M116.768598>
- Duffy, D., Rouilly, V., Libri, V., Hasan, M., Beitz, B., David, M., Urrutia, A., Bisiaux, A., LaBrie, S. T., Dubois, A., Boneca, I. G., Delval, C., Thomas, S., Rogge, L., Schmolz, M., Quintana-Murci, L., Albert, M. L., Abel, L., Alcover, A., ... Albert, M. L. (2014). Functional analysis via standardized whole-blood stimulation systems defines the boundaries of a healthy immune response to complex stimuli. *Immunity*, 40(3), 436–450. <https://doi.org/10.1016/j.immuni.2014.03.002>
- Feng, C., Stamos, N. M., Dragan, A. I., Medvedev, A., Whitford, M., Zhang, L., Song, C., Rallabhandi, P., Cole, L., Nhu, Q. M., Vogel, S. N., Geddes, C. D., & Cross, A. S. (2012). Sialyl residues modulate LPS-mediated signaling through the toll-like receptor 4 complex. *PLoS ONE*, 7(4), e32359. <https://doi.org/10.1371/journal.pone.0032359>
- Feng, C., Zhang, L., Almulki, L., Faez, S., Whitford, M., Hafezi-Moghadam, A., & Cross, A. S. (2011). Endogenous PMN sialidase activity exposes activation epitope on CD11b/CD18 which enhances its binding interaction with ICAM-1. *Journal of Leukocyte Biology*, 90(2), 313–321. <https://doi.org/10.1189/jlb.1210708>
- Glanz, V. Y., Myasoedova, V. A., Grechko, A. V., & Orekhov, A. N. (2019). Sialidase activity in human pathologies. *European Journal of Pharmacology*, 842, 345–350. <https://doi.org/10.1016/j.ejphar.2018.11.014>
- Guan, W., Ni, Z., Hu, Y., Liang, W., Ou, C., He, J., Liu, L., Shan, H., Lei, C. L., Hui, D. S. C., Du, B., Li, L. J., Zeng, G., Yuen, K. Y., Chen, R. C., Tang, C. L., Wang, T., Chen, P. Y., Xiang, J., ... China Medical Treatment Expert Group for Covid-19. (2020). Clinical characteristics of coronavirus disease 2019 in China. *New England Journal of Medicine*, 382(18), 1708–1720. <https://doi.org/10.1056/NEJMoa2002032>
- Guo, Q., Zhao, Y., Li, J., Liu, J., Yang, X., Guo, X., Kuang, M., Xia, H., Zhang, Z., Cao, L., Luo, Y., Bao, L., Wang, X., Wei, X., Deng, W., Wang, N., Chen, L., Chen, J., Zhu, H., ... You, F. (2021). Induction of alarmin S100A8/A9 mediates activation of aberrant neutrophils in the pathogenesis of COVID-19. *Cell Host & Microbe*, 29(2), 222–235.e4. <https://doi.org/10.1016/j.chom.2020.12.016>
- Henricks, P. A., Van Erne-van der Tol, M. E., & Verhoef, J. (1982). Partial removal of sialic acid enhances phagocytosis and the generation of superoxide and chemiluminescence by polymorphonuclear leukocytes. *Journal of Immunology*, 129, 745–750.
- Jutila, M. A., Rott, L., Berg, E. L., & Butcher, E. C. (1989). Function and regulation of the neutrophil MEL-14 antigen in vivo: Comparison with LFA-1 and MAC-1. *Journal of Immunology*, 143, 3318–3324.
- Knibbs, R. N., Goldstein, I. J., Ratcliffe, R. M., & Shibuya, N. (1991). Characterization of the carbohydrate binding specificity of the leucoagglutinating lectin from *Maackia amurensis*. Comparison with other sialic acid-specific lectins. *Journal of Biological Chemistry*, 266, 83–88. [https://doi.org/10.1016/S0021-9258\(18\)52405-4](https://doi.org/10.1016/S0021-9258(18)52405-4)
- Kuri-Cervantes, L., Pampena, M. B., Meng, W., Rosenfeld, A. M., Ittner, C. A. G., Weisman, A. R., Ageyuk, R. S., Mathew, D., Baxter, A. E., Vella, L. A., Kuthuru, O., Apostolidis, S. A., Bershaw, L., Dougherty, J., Greenplate, A. R., Pattekar, A., Kim, J., Han, N., Gouma, S., ... Betts, M. R. (2020). Comprehensive mapping of immune perturbations associated with severe COVID-19. *Science Immunology*, 5(49), eabd7114. <https://doi.org/10.1126/sciimmunol.abd7114>
- Leliefeld, P. H. C., Wessels, C. M., Leenen, L. P. H., Koenderman, L., & Pillay, J. (2016). The role of neutrophils in immune dysfunction during severe inflammation. *Critical Care*, 20, 73.
- Lilley, E., Stanford, S. C., Kendall, D. E., Alexander, S. P. H., Cirino, G., Docherty, J. R., George, C. H., Insel, P. A., Izzo, A. A., Ji, Y., Panettieri, R. A., Sobey, C. G., Stefanska, B., Stephens, G., Teixeira, M., & Ahluwalia, A. (2020). ARRIVE 2.0 and the British Journal of Pharmacology: Updated guidance for 2020. *British Journal of Pharmacology*, 177, 3611–3616. <https://doi.org/10.1111/bph.15178>
- Lipničanová, S., Chmelová, D., Ondrejovič, M., Frečer, V., & Miertuš, S. (2020). Diversity of sialidases found in the human body—A review. *International Journal of Biological Macromolecules*, 148, 857–868. <https://doi.org/10.1016/j.ijbiomac.2020.01.123>
- Liu, J., Zhang, S., Wu, Z., Shang, Y., Dong, X., Li, G., Zhang, L., Chen, Y., Ye, X., Du, H., Liu, Y., Wang, T., Huang, S., Chen, L., Wen, Z., Qu, J., & Chen, D. (2020). Clinical outcomes of COVID-19 in Wuhan, China: A large cohort study. *Annals of Intensive Care*, 10(1), 99. <https://doi.org/10.1186/s13613-020-00706-3>
- Macauley, M. S., Crocker, P. R., & Paulson, J. C. (2014). Siglec-mediated regulation of immune cell function in disease. *Nature Reviews Immunology*, 14, 653–666. <https://doi.org/10.1038/nri3737>
- Messerer, D. A. C., Vidoni, L., Erber, M., Stratmann, A. E. P., Bauer, J. M., Braun, C. K., Hug, S., Adler, A., Nilsson Ekdahl, K., Nilsson, B., Barth, E., Radermacher, P., & Huber-Lang, M. (2020). Animal-free human whole blood sepsis model to study changes in innate immunity. *Frontiers in Immunology*, 11, 571992. <https://doi.org/10.3389/fimmu.2020.571992>
- Mills, E. L., Debets-Ossenkopp, Y., Verbrugh, H. A., & Verhoef, J. (1981). Initiation of the respiratory burst of human neutrophils by influenza virus. *Infection and Immunity*, 32, 1200–1205. <https://doi.org/10.1128/iai.32.3.1200-1205.1981>
- Mittal, M., Siddiqui, M. R., Tran, K., Reddy, S. P., & Malik, A. B. (2014). Reactive oxygen species in inflammation and tissue injury. *Antioxidants & Redox Signaling*, 20, 1126–1167. <https://doi.org/10.1089/ars.2012.5149>
- Mócsai, A. (2013). Diverse novel functions of neutrophils in immunity, inflammation, and beyond. *Journal of Experimental Medicine*, 210, 1283–1299. <https://doi.org/10.1084/jem.20122220>
- Movsisyan, L. D., & Macauley, M. S. (2020). Structural advances of Siglecs: Insight into synthetic glycan ligands for immunomodulation. *Organic and Biomolecular Chemistry*, 18, 5784–5797. <https://doi.org/10.1039/DO0B01116A>

- Percie du Sert, N., Hurst, V., Ahluwalia, A., Alam, S., Avey, M. T., Baker, M., Browne, W. J., Clark, A., Cuthill, I. C., Dirnagl, U., Emerson, M., Garner, P., Holgate, S. T., Howells, D. W., Karp, N. A., Lazic, S. E., Lidster, K., MacCallum, C. J., Macleod, M., ... Würbel, H. (2020). The ARRIVE guidelines 2.0: Updated guidelines for reporting animal research. *PLoS Biology*, 18(7), e3000410. <https://doi.org/10.1371/journal.pbio.3000410>
- Petri, B., Phillipson, M., & Kubes, P. (2008). The physiology of leukocyte recruitment: An in vivo perspective. *Journal of Immunology*, 180, 6439–6446. <https://doi.org/10.4049/jimmunol.180.10.6439>
- Pshezhetsky, A. V., & Hinek, A. (2011). Where catabolism meets signalling: Neuraminidase 1 as a modulator of cell receptors. *Glycoconjugate Journal*, 28, 441–452. <https://doi.org/10.1007/s10719-011-9350-5>
- Rhodes, A., Evans, L. E., Alhazzani, W., Levy, M. M., Antonelli, M., Ferrer, R., Kumar, A., Sevransky, J. E., Sprung, C. L., Nunnally, M. E., Rochwerf, B., Rubenfeld, G. D., Angus, D. C., Annane, D., Beale, R. J., Bellinhan, G. J., Bernard, G. R., Chiche, J. D., Coopersmith, C., ... Dellinger, R. P. (2017). Surviving Sepsis Campaign: International guidelines for management of sepsis and septic shock: 2016. *Intensive Care Medicine*, 43(3), 304–377. <https://doi.org/10.1007/s00134-017-4683-6>
- Rifat, S., Kang, T. J., Mann, D., Zhang, L., Puche, A. C., Stamatou, N. M., Goldblum, S. E., Brossmer, R., & Cross, A. S. (2008). Expression of sialyltransferase activity on intact human neutrophils. *Journal of Leukocyte Biology*, 84(4), 1075–1081. <https://doi.org/10.1189/jlb.0706462>
- Rittirsch, D., Huber-Lang, M. S., Flierl, M. A., & Ward, P. A. (2009). Immunodesign of experimental sepsis by cecal ligation and puncture. *Nature Protocols*, 4, 31–36. <https://doi.org/10.1038/nprot.2008.214>
- Sakarya, S. (2004). Mobilization of neutrophil sialidase activity desialylates the pulmonary vascular endothelial surface and increases resting neutrophil adhesion to and migration across the endothelium. *Glycobiology*, 14, 481–494. <https://doi.org/10.1093/glycob/cwh065>
- Schmidt, T., Zündorf, J., Gröger, T., Brandenburg, K., Reiners, A.-L., Zinserling, J., & Schnitzler, N. (2012). CD66b overexpression and homotypic aggregation of human peripheral blood neutrophils after activation by a gram-positive stimulus. *Journal of Leukocyte Biology*, 91(5), 791–802. <https://doi.org/10.1189/jlb.0911483>
- Schulte-Schrepping, J., Reusch, N., Paclik, D., Baßler, K., Schlickeiser, S., Zhang, B., Krämer, B., Krammer, T., Brumhard, S., Bonaguro, L., de Domenico, E., Wendisch, D., Grasshoff, M., Kapellos, T. S., Beckstette, M., Pecht, T., Saglam, A., Dietrich, O., Mei, H. E., ... Ziebuhr, J. (2020). Severe COVID-19 is marked by a dysregulated myeloid cell compartment. *Cell*, 182(6), 1419–1440.e23. <https://doi.org/10.1016/j.cell.2020.08.001>
- Segal, A. W. (2005). How neutrophils kill microbes. *Annual Review of Immunology*, 23, 197–223. <https://doi.org/10.1146/annurev.immunol.23.021704.115653>
- Sheu, C.-C., Gong, M. N., Zhai, R., Chen, F., Bajwa, E. K., Clardy, P. F., Gallagher, D. C., Thompson, B. T., & Christiani, D. C. (2010). Clinical characteristics and outcomes of sepsis-related vs non-sepsis-related ARDS. *Chest*, 138(3), 559–567. <https://doi.org/10.1378/chest.09-2933>
- Silvin, A., Chapuis, N., Dunsmore, G., Goubet, A.-G., Dubuisson, A., Derosa, L., Almire, C., Hénon, C., Kosmider, O., Droin, N., Rameau, P., Catelain, C., Alfaro, A., Dussiau, C., Friedrich, C., Sourdeau, E., Marin, N., Szwebel, T. A., Cantin, D., ... Solary, E. (2020). Elevated calprotectin and abnormal myeloid cell subsets discriminate severe from mild COVID-19. *Cell*, 182(6), 1401–1418.e18. <https://doi.org/10.1016/j.cell.2020.08.002>
- Smutova, V., Albohy, A., Pan, X., Korchagina, E., Miyagi, T., Bovin, N., Cairo, C. W., & Pshezhetsky, A. V. (2014). Structural basis for substrate specificity of mammalian neuraminidases. *PLoS ONE*, 9(9), e106320. <https://doi.org/10.1371/journal.pone.0106320>
- Sônego, F., Castanheira, F. V., Ferreira, R. G., Kanashiro, A., Leite, C. A., Nascimento, D. C., Colon, D. F., Borges, V. D., Alves-Filho, J. C., & Cunha, F. Q. (2016). Paradoxical roles of the neutrophil in sepsis: Protective and deleterious. *Frontiers in Immunology*, 7, 1–7.
- Spiller, F., Carlos, D., Souto, F. O., de Freitas, A., Soares, F. S., Vieira, S. M., Paula, F. J. A., Alves-Filho, J. C., & Cunha, F. Q. (2012). α 1-Acid glycoprotein decreases neutrophil migration and increases susceptibility to sepsis in diabetic mice. *Diabetes*, 61(6), 1584–1591. <https://doi.org/10.2337/db11-0825>
- Spiller, F., Orrico, M. I. L., Nascimento, D. C., Czaikoski, P. G., Souto, F. O., Alves-Filho, J. C., Freitas, A., Carlos, D., Montenegro, M. F., Neto, A. F., Ferreira, S. H., Rossi, M. A., Hothersall, J. S., Assreuy, J., & Cunha, F. Q. (2010). Hydrogen sulfide improves neutrophil migration and survival in sepsis via K^+ ATP channel activation. *American Journal of Respiratory and Critical Care Medicine*, 182(3), 360–368. <https://doi.org/10.1164/rccm.200907-1145OC>
- Steevens, T. A. M., & Meyaard, L. (2011). Immune inhibitory receptors: Essential regulators of phagocyte function. *European Journal of Immunology*, 41, 575–587. <https://doi.org/10.1002/eji.201041179>
- Suzuki, H., Kurita, T., & Kakinuma, K. (1982). Effects of neuraminidase on O_2 consumption and release of O_2 and H_2O_2 from phagocytosing human polymorphonuclear leukocytes. *Blood*, 60, 446–453. <https://doi.org/10.1182/blood.V60.2.446.446>
- Tan, J., Yuan, Y., Xu, C., Song, C., Liu, D., Ma, D., & Gao, Q. (2021). A retrospective comparison of drugs against COVID-19. *Virus Research*, 294, 198262. <https://doi.org/10.1016/j.virusres.2020.198262>
- Tan, Q., Duan, L., Ma, Y., Wu, F., Huang, Q., Mao, K., Xiao, W., Xia, H., Zhang, S., Zhou, E., Ma, P., Song, S., Li, Y., Zhao, Z., Sun, Y., Li, Z., Geng, W., Yin, Z., & Jin, Y. (2020). Is oseltamivir suitable for fighting against COVID-19: In silico assessment, in vitro and retrospective study. *Bioorganic Chemistry*, 104, 104257. <https://doi.org/10.1016/j.bioorg.2020.104257>
- Varki, A. (2008). Sialic acids in human health and disease. *Trends in Molecular Medicine*, 14, 351–360. <https://doi.org/10.1016/j.molmed.2008.06.002>
- Varki, A., & Gagneux, P. (2012). Multifarious roles of sialic acids in immunity. *Annals of the New York Academy of Sciences*, 1253, 16–36. <https://doi.org/10.1111/j.1749-6632.2012.06517.x>
- Veras, F. P., Pontelli, M. C., Silva, C. M., Toller-Kawahisa, J. E., de Lima, M., Nascimento, D. C., Schneider, A. H., Caetité, D., Tavares, L. A., Paiva, I. M., Rosales, R., Colón, D., Martins, R., Castro, I. A., Almeida, G. M., Lopes, M. I. F., Benatti, M. N., Bonjorno, L. P., Giannini, M. C., ... Cunha, F. Q. (2020). SARS-CoV-2-triggered neutrophil extracellular traps mediate COVID-19 pathology. *Journal of Experimental Medicine*, 217(12), e20201129. <https://doi.org/10.1084/jem.20201129>
- Vimr, E. R., & Troy, F. A. (1985). Identification of an inducible catabolic system for sialic acids (nan) in *Escherichia coli*. *Journal of Bacteriology*, 164, 845–853. <https://doi.org/10.1128/jb.164.2.845-853.1985>
- Vogl, T., Stratis, A., Wixler, V., Völler, T., Thurainayagam, S., Jorch, S. K., Zenker, S., Dreiling, A., Chakraborty, D., Fröhling, M., Paruzel, P., Wehmeyer, C., Hermann, S., Papanonopoulou, O., Geyer, C., Loser, K., Schäfers, M., Ludwig, S., Stoll, M., ... Roth, J. (2018). Autoinhibitory regulation of S100A8/S100A9 alarmin activity locally restricts sterile inflammation. *Journal of Clinical Investigation*, 128(5), 1852–1866. <https://doi.org/10.1172/JCI89867>
- Wang, T., du, Z., Zhu, F., Cao, Z., An, Y., Gao, Y., & Jiang, B. (2020). Comorbidities and multi-organ injuries in the treatment of COVID-19. *The Lancet*, 395(10228), e52. [https://doi.org/10.1016/S0140-6736\(20\)30558-4](https://doi.org/10.1016/S0140-6736(20)30558-4)
- Wilk, A. J., Rustagi, A., Zhao, N. Q., Roque, J., Martínez-Colón, G. J., McKechnie, J. L., Ivison, G. T., Ranganath, T., Vergara, R., Hollis, T., Simpson, L. J., Grant, P., Subramanian, A., Rogers, A. J., & Blish, C. A. (2020). A single-cell atlas of the peripheral immune response in

- patients with severe COVID-19. *Nature Medicine*, 26(7), 1070–1076. <https://doi.org/10.1038/s41591-020-0944-y>
- Witko-Sarsat, V., Mocek, J., Bouayad, D., Tamassia, N., Ribeil, J.-A., Candalh, C., Davezac, N., Reuter, N., Mouthon, L., Hermine, O., Pederzoli-Ribeil, M., & Cassatella, M. A. (2010). Proliferating cell nuclear antigen acts as a cytoplasmic platform controlling human neutrophil survival. *Journal of Experimental Medicine*, 207(12), 2631–2645. <https://doi.org/10.1084/jem.20092241>
- Worthen, G. S., Schwab, B., Elson, E. L., & Downey, G. P. (1989). Mechanics of stimulated neutrophils: Cell stiffening induces retention in capillaries. *Science*, 245, 183–186. <https://doi.org/10.1126/science.2749255>
- Yang, W. H., Heithoff, D. M., Aziz, P. V., Haslund-Gourley, B., Westman, J. S., Narisawa, S., Pinkerton, A. B., Millán, J. L., Nizet, V., Mahan, M. J., & Marth, J. D. (2018). Accelerated aging and clearance of host anti-inflammatory enzymes by discrete pathogens fuels sepsis. *Cell Host & Microbe*, 24(4), 500–513.e5. <https://doi.org/10.1016/j.chom.2018.09.011>

SUPPORTING INFORMATION

Additional supporting information can be found online in the Supporting Information section at the end of this article.

How to cite this article: de Oliveira Formiga, R., Amaral, F. C., Souza, C. F., Mendes, D. A. G. B., Wanderley, C. W. S., Lorenzini, C. B., Santos, A. A., Antônia, J., Faria, L. F., Natale, C. C., Paula, N. M., Silva, P. C. S., Fonseca, F. R., Aires, L., Heck, N., Starick, M. R., Queiroz-Junior, C. M., Santos, F. R. S., de Souza, F. R. O., ... Spiller, F. (2023). Neuraminidase is a host-directed approach to regulate neutrophil responses in sepsis and COVID-19. *British Journal of Pharmacology*, 1–22. <https://doi.org/10.1111/bph.16013>